



KYOTO SANGYO UNIVERSITY
DIVISION OF FRONTIER INFORMATICS

DOCTORAL DEGREE THESIS

Spatial-Temporal Processing in Rasterized Map
Tile based on Social Media Data with Geolocation
–Applications of POIs and User Behavior Analysis based on Dynamic Feature Extraction–

Author:
Xie Huaze

Supervisor:
Kawai Yukiko

Co-Supervisor:
Wang Yuanyuan

A thesis submitted in fulfillment of the requirements for the

Doctoral Dissertation in Computer Science

in the

Department of Computer Science
Intelligent Informatics Section

July, 2022

Contents

I	Approach	1
1	Introduction	3
1.1	Background	3
1.2	Motivation	4
1.3	Approach	4
1.4	Contribution	5
1.5	Thesis Overview	6
1.6	Organization of the Thesis	6
2	Geographical Information	7
2.1	Chapter Overview	7
2.2	Web Map	8
2.3	Map Tile	9
2.4	Raster Map	10
2.5	Related Work	11
2.5.1	Geo-Social Media Data Representation	11
2.5.2	Application of Map Zooming and Examples	12
2.5.3	Application of Regional Competitiveness and Examples	14
3	Problems and Solutions	17
3.1	Chapter Overview	17
3.2	Problems	17
3.3	Map Tile Selection	18
3.4	Map Rasterization	18
3.5	MRSS	20
3.6	Comparative Experiment	22
3.7	Result	23
3.8	Conclusion and Discussion	24
II	Applications	25
4	Application I: Map Zooming Processing	27
4.1	Chapter Overview	27
4.2	Background	28
4.3	Data Collection	29
4.4	Raster Processing	30

4.5	Framework: SZ-GAT	31
4.5.1	Process Overview	31
4.5.2	MRSS for Zooming	32
4.5.3	Graph Structure	33
4.5.4	Global Attention Mechanism	34
4.5.5	Map Zooming Process	35
4.6	Evaluation and Experiment	36
4.6.1	Settings	36
4.6.2	Dataset	37
4.6.3	Baselines	37
4.6.4	Evaluation Results	39
4.6.5	Case Study	40
4.7	Conclusion and Discussion	41
5	Application II: Regional Competitiveness	43
5.1	Chapter Overview	43
5.2	Background	44
5.3	Framework: RC-GAT	45
5.3.1	Process Overview	45
5.3.2	Rasterized Competitiveness	45
5.3.3	Temporal Feature	47
5.4	Evaluation and Experiment	48
5.4.1	Settings	48
5.4.2	Dataset	49
5.4.3	Baselines	49
5.4.4	Evaluation Results	50
5.4.5	Visualization	53
5.5	Conclusion and Discussion	55
III	Summary	57
6	Discussion	59
6.1	Conclusion	59
6.2	Discussion	59
6.3	Future Work	61
	Bibliography	61
	List of Figures	68

List of Tables	69
Acknowledgements	70

Part I

Approach

1 Introduction

Chapter Contents

1.1	Background	3
1.2	Motivation	4
1.3	Approach	4
1.4	Contribution	5
1.5	Thesis Overview	6
1.6	Organization of the Thesis	6

1.1 Background

Owing to the increasing popularity of social media services, mobile terminals have enabled the public to share their daily activities online and leave their digital footprint in urban areas. The information available on social media reflects the real-time characteristics (flows, services, scenery, and parking) of urban facilities such as restaurants, transportation, and attractions. GPS coordinates within urban areas collected by geo-tagged social-media messages help researchers understand dynamic spatially oriented human activities and urban spatial patterns.

This thesis introduces **a multidisciplinary theme to develop advanced raster maps statistically**. The computational training techniques for geolocation-related data analysis will be discussed along with feature extraction from regional feature information on raster maps. Regional feature information will provide a rigorous foundation to address a wide range of applications including disease mapping, emerging infectious diseases, ecological landscape assessment, user visit trends from social networks, regional competitiveness extraction, raster feature assessment, and map accuracy assessment.

An advanced raster map analysis system will be developed to integrate these techniques with an advanced visualization toolbox and use the system to conduct large case studies using rich sets of raster data, primarily from user-based social media. As a result, it will be possible to study and evaluate raster maps of societal, ecological, and environmental variables to facilitate quantitative characterization and comparative analysis of geo-spatial trends, patterns, and phenomena. In addition to environmental studies, these techniques and tools can be used for policy decisions at local, state, and national levels, crisis management, and planning of infrastructure.

1.2 Motivation

Geo-spatial data form the foundation of an information-based society. Consider an imminent 21st-century scenario: A message passing with multi-categorical map contains the problem of POI visualization represents. What kind of visualization of the map scale, level of detail should be adopted? The spatial pattern of the map reveals the societal, ecological, and environmental conditions of the landscape.

The motivation of this research is to developed a spatial-temporal map visualization system with geo-tagged social media data distribution.

Spatial Representation contains the 3D location of places. However, in this thesis, the height dimension Z axis is ignored, and a 2D flat map on the X-Y axis with a new dimension "Zoom" of the web map compose the 3D base map.

Temporal Representation contains the dynamic changes on the map with monthly timelines of Tweets and utilizes a user visit dataset to map to POI attributes.

1.3 Approach

a. Raster Units Representation

Compared with the traditional placemark visualization and feature extraction model, the original POI relationship learning model (such as POI facility feature clustering, POI recommendation with categories, etc.) is improved to the POI fully connected with neighboring raster units, and POI visualization with dynamic user visits attributes on the temporal raster map tiles.

b. Integration of Map Rasterization Analysis

This thesis contains the review the methodological conduct and reporting of user behavior prediction models for predicting the user preference of POI visits or the reflection of government measures since COVID-19.

c. POI with User Visit Prediction Model

The Twitter with geolocation data is used to import on the Kyoto map and map the Tweet attributes to related POIs. Then, SZ-GAT and RC-GAT frameworks are utilized to predict the raster unit feature of user preference combine with POI information.

d. Dynamic Visualization

The visualization is based on Google map and Open Street Map (OSM) and show the dynamic results on the time line from Jan 2020 to Dec 2021.

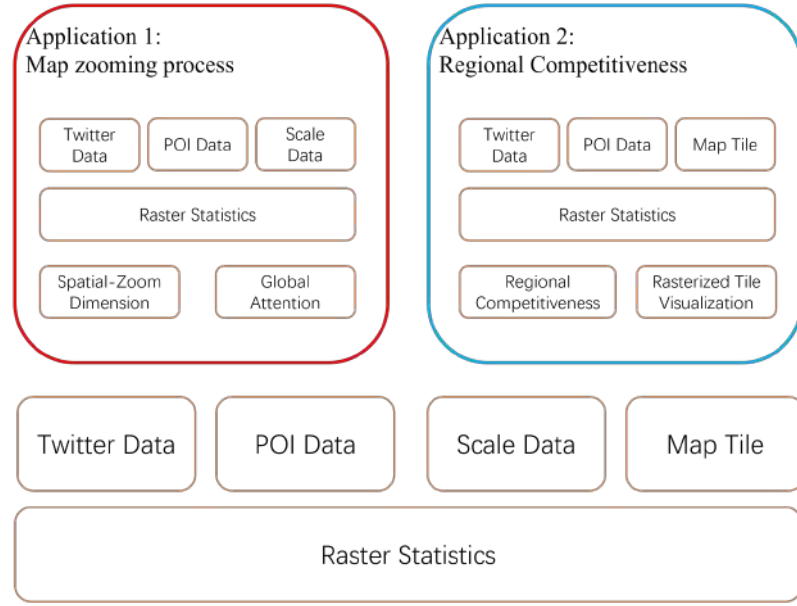


Figure 1.1: The overview of proposed raster statistics method and applications.

1.4 Contribution

a. Map Rasterization Statistics System (MRSS)

A map rasterization statistics system is proposed in this thesis, and MRSS is a significant contribution to POI data analysis contains raster map feature extraction and POI mapping with coordinates such as the overview shown in Figure 1.1.

b. Map Zooming Dimension Processing

A POI training model is proposed to visualize the placemark with user preference at multiple scales. A global POI category attention mechanism is contributed based on social data and map zooming levels.

c. Regional Competitiveness Processing

A visit category training model is developed based on a raster-competitive user database from Tweets and POIs. A category analysis is contributed the impact of government policy on user visit categories since COVID-19.

d. Graph Attention Networks and Variants

The experiments and evaluation of the proposed frameworks are completed on Kyoto map data with SZ-GAT and RC-GAT.

1.5 Thesis Overview

In this thesis, a map rasterization statistics system (MRSS) will be introduced. MRSS contains the data from Twitter, POI, map zooming detail, and map tiles shown in Figure 1.1. And MRSS contains the task of short text semantic analysis from Twitter, POI attributes rasterization, and POI features with user visit information map to the raster units.

MRSS will be applied to the application of map zooming processing and regional competitiveness processing with the Graph Attention Network (GAT) model. GAT training model is easily adaptable to any short message training and POI-related prediction test in order to solve some visualization problems and offer proposals for urban facility function prediction. The map visualization will be introduced by Twitter data analysis from the GAT training method, and the POI attributes of the user's description from Tweets will be used to train the POI data set of each raster unit which has the same data characteristic spatial distribution [1].

1.6 Organization of the Thesis

This thesis is organized as follows:

1. **Chapter 2** is the overview and related work of this thesis, describing in detail the importance of rasterized map tile processing and the main problems encountered.
2. **Chapter 3** contains the problem and solution in this thesis. A comparative experiment introduces the performance of POI extraction on MRSS.
3. **Chapter 4** contains the application of the map zooming process. A spatial zooming graph attention framework is proposed to visualize the POI of user preference.
4. **Chapter 5** introduces an application of the regional competitiveness process. A category analysis method is proposed to train the impact of government policy on user access categories since COVID-19.
5. **Chapter 6** is the discussion and conclusion of this research and the future work of this thesis is also introduced in this chapter.

2 Geographical Information

*Understanding Multilingual Correlation of Geo-Tagged Tweets
for POI Recommendation*

– Wang, Yuanyuan, et al.

Chapter Contents

2.1	Chapter Overview	7
2.2	Web Map	8
2.3	Map Tile	9
2.4	Raster Map	10
2.5	Related Work	11
2.5.1	Geo-Social Media Data Representation	11
2.5.2	Application of Map Zooming and Examples	12
2.5.3	Application of Regional Competitiveness and Examples	14

2.1 Chapter Overview

In this thesis, a **map rasterization statistics system (MRSS)** is introduced to thematic coding of POI attributes with user visit history from social media data conducted as part of rasterized geographical information analysis research. The proposed MRSS framework is easily **adaptable to any short message sampling with geolocation and POI-related prediction test** in order to solve some visualization problems and offer proposals for urban facility function prediction. The map visualization will be purposed by Twitter data geo-tags analysis with MRSS, and the POI attributes of the user's description from Tweets will be used to train the POI data set of each raster unit which has the same data Characteristic Spatial Distribution (CSD) with training data [1].

Our research focuses on the **task of separating between Tweets data and POI features** at first (shown in Figure 2.1). And after having successfully acquired the POI attribute relations from Tweets, the category relation between POI and Tweets attributes is used to predict the POI spatial feature with the same category and the dynamic changing of temporal raster maps.

In addition, the related work of map zooming dimension and map scales are introduced in this thesis to observe the relation between user preference and regional competitiveness combined with Tweets and POIs [2].

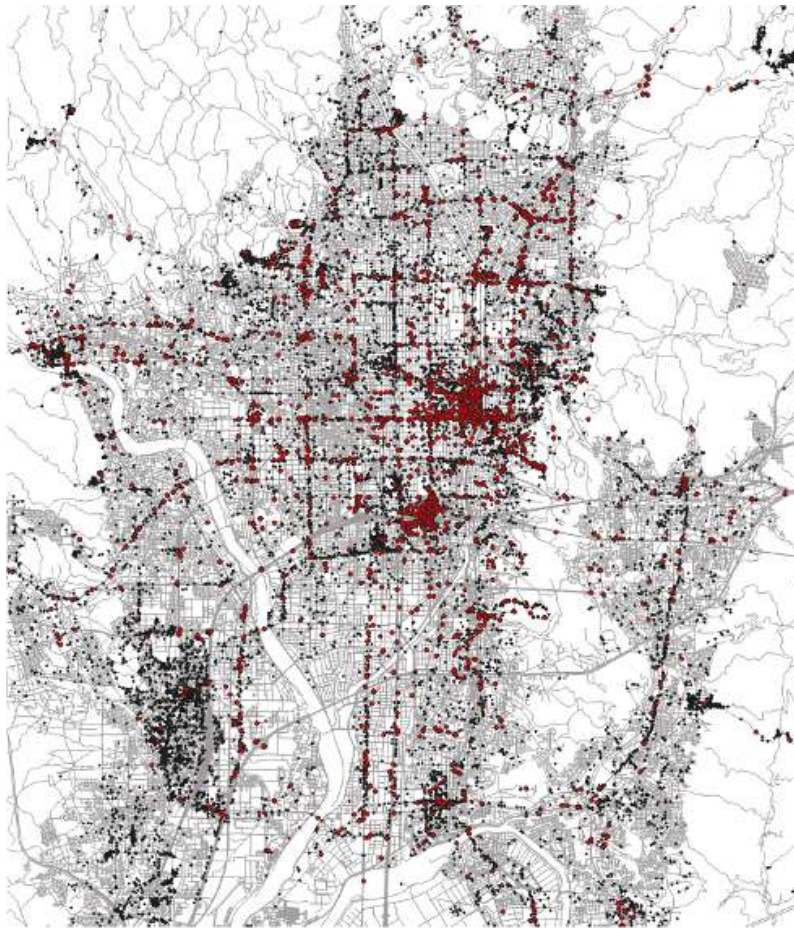


Figure 2.1: The visualization of POIs (black dots) and Twitter data (red dots) on the Kyoto City road map.

2.2 Web Map

Web maps are a common interactive display platform for geographic information, and the events described by this geographic information are often used for spatial feature analysis. For the common flat Google Map, **geographic information is composed of multiple layers of points, lines, and surface features**, which together form scalable location information. Map layers contain multi-dimensional geographic information, such as road layers, building layers, river layers, traffic layers, and more.

A web map consists of a base map, a set of data layers (many data layers contain interactive pop-ups that display information about the data), an extent, and navigation tools for panning and zooming. Typically, base maps and layers are hosted and shared through a set of divisible map tiles. In Figure 2.1, the **Kyoto City Road Map with POIs** (black dots) and a set of **Twitter data** (red dots) are introduced.

To provide context shown in Figure 2.2, the web map also has a topographic base

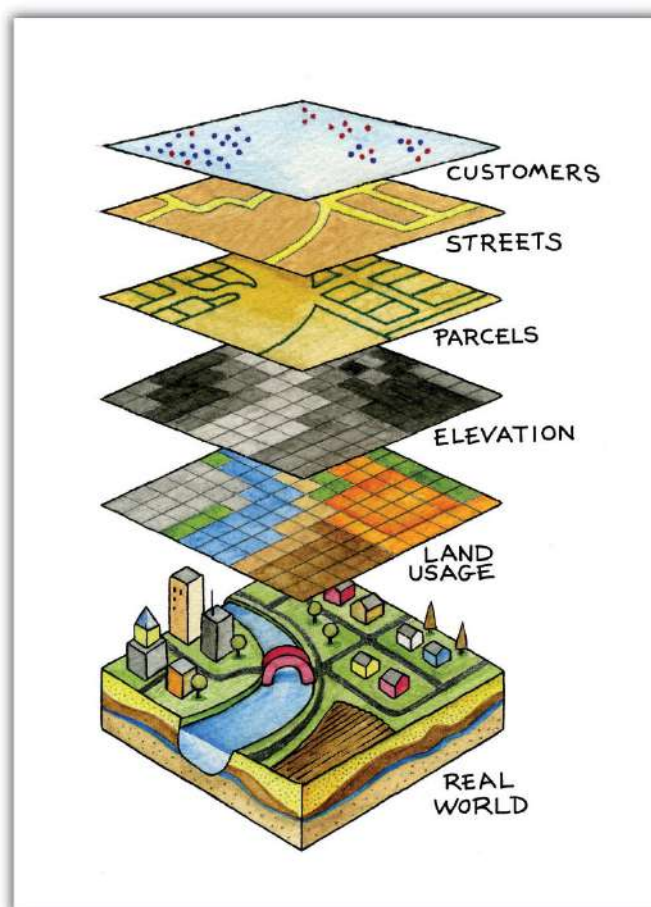


Figure 2.2: The visualization of map layers of the flat web maps.

map, which includes shaded relief imagery of cities, roads, and buildings superimposed on the land cover [3]. The map layer of the flat web maps contains the Customer Layer, Streets Layer, Parcels Layer, Elevation Layer, and Land Usage Layer. Where the **raster map layer is composed of Elevation Layer and Land Usage Layer**.

2.3 Map Tile

A tiled web map is a map displayed in a web browser by seamlessly joining dozens of individually requested image or vector data files. It is the most popular way to display and navigate maps, replacing other methods such as Web Map Service (WMS) which typically display a single large image, with arrow buttons to navigate to nearby areas. Google Maps was one of the first major mapping sites to use this technique such as Figure 2.3. The first tiled web maps used raster tiles, before the emergence of vector tiles.

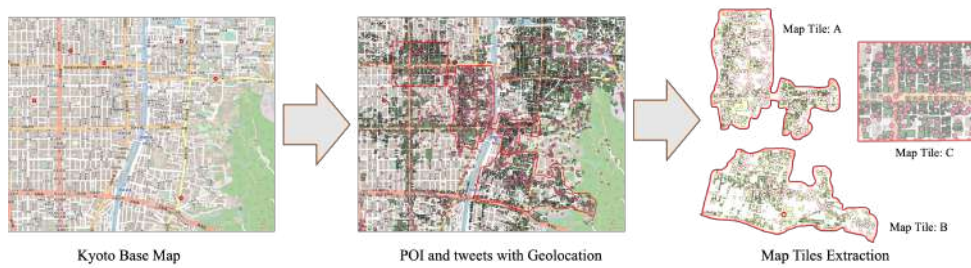


Figure 2.3: The process of map tiles extraction from Google Map API.

There are several advantages to tiled maps. Each time the user pans, most of the tiles are still relevant and can be kept displayed, while new tiles are fetched. This greatly improves the user experience, compared to fetching a single map image for the whole view-port. It also allows individual tiles to be pre-computed, a task easy to parallelize. Also, displaying rendered images served from a web server is less computationally demanding than rendering images in the browser, a benefit over technologies such as Web Feature Service (WFS). While many map tiles are in raster format (a bitmap file such as PNG or JPG), the number of suppliers of vector tiles is growing. Vector tiles are rendered by the client browser, which can thus add a custom style to the map. Vector map tiles may also be rotated separately from any text overlay so that the text remains readable.

2.4 Raster Map

In this research, the distribution of POIs on the map is uneven, and blank maps waste a lot of computing resources. In this thesis, the rasterized map tile is adopted to complete the regional competitive prediction and focus on the POI dense cores map tile.

Map tile originated from a technology called “slippy map”, which makes maps more accessible and load more quickly in 2005[4]. Since 2005, the map was no longer a single image; however, several images were joined together seamlessly. Interaction with the map only requires the necessary sections of the map to be loaded and displayed, and not the entire image [5]. The images were called raster tiles, and all major map applications and software libraries used Google’s method [6].

This thesis is based on the ordinary 2D flat web map, **the location attribute of the POI is described by the latitude and longitude, or the plane distance on the X-Y axis**. The Kyoto map is divided into a set of grids and constructed square map tiles. As shown in Figure 2.4, a raster base map with POIs is introduced which is divided into a set of grids using the Mercator projection system. **Each cell on the map tile is called a raster unit, and all units share a data-storage scheme on a map tile**. The schemes

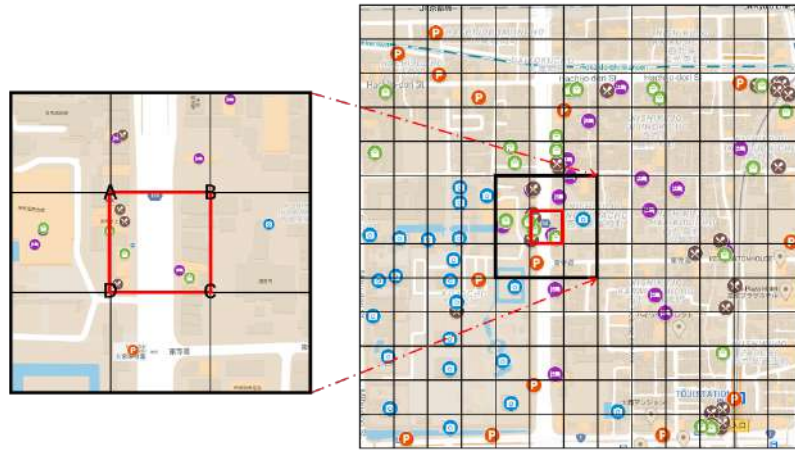


Figure 2.4: An example of a basic raster unit (red area) on the Google map tile.

are described as having the same parameters, such as the grid pixel size, tile shape and size, coordinate system origin, tile matrix size, and the map scales. The raster map tiles obey the Web Map Tile Service (WMTS) standard definition from the Open Geo-spatial Consortium (OGC) [7].

Raster data is usually used in geographic information analysis to describe satellite imagery and multi-element measurement distribution (rainfall, thermal imaging, slope, etc.) [6]. This raster model is chosen to be able to quantify and describe the densely populated core of the city as competitive with five POI attributes. To estimate the spatial variation of competitiveness in the area on the map, **POI attributes of each raster unit are represented by 5 POI categories** from Tweets shown in Figure 2.4 including the restaurant (only dine-in restaurants were counted), shops (convenience stores, markets, malls), transportations (parking, bus stations, train stations, airports), attractions and hotels. With the distribution of POI attributes on the map tiles, the raster unit features can be labeled with Tweet categories initially.

2.5 Related Work

2.5.1 Geo-Social Media Data Representation

Social media data as a user has a long-term development in daily life, product experience, preference analysis, and dynamic monitoring. Social media data, such as Twitter and Weibo, is used by many researchers in the areas of recommendation systems, data security, and geographic information analysis. User preference dynamics can be extracted with a joint decomposition model of the user's behavioral patterns and generate recommendations or predict the user's purchasing trend. The user preference dynamic

model provides ideas for our research.

In terms of geographic information analysis, the geographic location information attached to social media data has become the most popular research object. Combining POI data and map information, researchers can analyze natural events, disaster management, and historical information in a specific area from the perspective of big data. The GNN model achieved better performance on the featured trend between tiles and can understand the location features in the geographic environment through training. In geographic information analysis, both POI data and social data are unstructured text labels. The graph structure with attention module can complete the dynamics of the block features. In order to analyze social data over time or geographic spatial movement, a spatio-temporal graph attention network is proposed. This method is conducive for the change of text features on map tiles over time and improves the ability of labels to describe the spatial features of the tiles. In this thesis, a spatio-temporal attention network is used for feature description and competitiveness analysis between map tiles of different categories.

2.5.2 Application of Map Zooming and Examples

Map zooming with POIs priority visualization concentrate on the user's preferred attributes of POI. The POI contains various user information and place characteristics [8], which are two research points: (a) from users to placemarks, and (b) from placemarks to users. A study [9] introduced geolocation prediction (GP) and reviewed the two research points as user-profiling-based and content-based geolocation prediction.

(a). Users to placemarks represent a series of studies based on the text-feature-analysis method containing user location information and extended to placemark attribute analysis on the map [1] [2]. The authors demonstrated the visualization of user-shared placemark map tiles for application to natural events and human-change-predictive tasks [3]. This method is used to construct recommendation algorithms for POIs by extracting user characteristics and inferring user preferences based on object attributes. A previous study on spatial-temporal neural networks achieved excellent results on raster map tiles with user location-related geographic information [7] [10]. The abovementioned studies demonstrate the feasibility of the location information shared by users, and the related geographic placemark attributes are learnable [11].

(b). Placemarks to users utilize the placemark-feature distribution on a map to describe fixed-region attributes. Social-media data can be used to verify the prediction accuracy with different dimensions in a map tile [12]. For a certain map tile, the included multiple POI features depend on the observed attributes and the location features of ad-

jacent POI data, thereby inferring the unknown attributes of a geographic location [13]. Some difficulties are associated with the quality of POI annotations and the relevance of social-media data to geographic locations [14].

In previous studies on 2D or 3D flat maps, the spatial problems of fixed distance or fixed position between POIs were solved using a basic map with a fixed scale and zoom level. For example, the efficient destination retrieval for a query to POIs [15], incremental POI nodes mapping between large graph structures [16], and traffic flow prediction [17] are all adopted spatial-temporal frameworks with a learnable positional attention mechanism. However, the geographic information in these studies is aggregated from a priori maps with fixed zoom levels. The map zoom level as a controlled variable is currently only introduced in the geographic information systems field. On the one hand, the POI data generalization technique changes the degree of abstraction of map content. Content zooming provides the user with the capability to change the amount and the granularity of foreground information presented while maintaining the geometric map scale [18]. Content zooming allows overriding the effects of standard map generalization, focusing on optimized content representation to aid the information-seeking task of a mobile user. On the other hand, matching spatial data at different map scales for integrating, evaluating, and updating spatial data were collected and maintained at various scales. A relaxation labeling technique to match the areal features and/or for a different scale range with a contextual approach was proposed [19]. More related to our research is the development of a web map service platform to browse the user behavior modeling and extract regions of interest with multiple map scales [20]. The platform utilizes the user's zoom-in map operations to indicate increasing interest. In contrast, the zoom-out indicates decreasing interest. A new hierarchical Gaussian mixture model to model the multi-granular spatial structure and extract browsing interests was also proposed. For our research, the map zooming process is used to reflect the POI visit history with social media and user preference on the raster maps. This is the first time that map zoom level has been applied as a map dimension to a graph structure framework.

For POI filtering, we focus on recommending a ranked set of POIs for a user where the POI after map zooming should be the one preferred by the user. A model was proposed to learn content-aware POI embeddings through user visit sequences and POI textual information [21]. A category-aware gated recurrent unit model has been proposed to mitigate the negative impact of sparse check-in data, capture long-range dependence between user check-ins and get better recommendation results of POI category [22]. An interactive multi-task learning framework has been proposed to exploit the interplay between activity and location preference with temporal-aware activity encoder [23]. In our previous research, we constructed the POI data set with text categories for regional

competitiveness training, which contain the POI data with social media records and user preference distributions [24].

The proposed model exhibits several significant differences. First, we focus on learnable POI graph representations through a graph attention network (GAT) and zooming process analysis. The dynamic-location-space changes in the POI attributes are described by the map-zooming process. Therefore, the proposed method exhibits differences in the optimization goals of the algorithm and zooming dimensions. Second, the graph structure in the proposed method was improved for spatial zooming. Third, the learnable POIs in the zooming-evaluation process was imported from a different resource, and the predictive results of the proposed model effectively described the hiding and appearance of POIs during map zooming.

2.5.3 Application of Regional Competitiveness and Examples

Social media data as a user has a long-term development in daily life, product experience, preference analysis, and dynamic monitoring [25] [26]. Social media data, such as Twitter and Weibo, is used by many researchers in the areas of recommendation systems, data security, and geographic information analysis [27]. User preference dynamics, by extracting a joint decomposition model of the user's time pattern to generate recommendations, to predict the user's buying trend [28] [29]. The user preference dynamic model provides ideas for our research. In the past 2020, many researchers used social media data to observe the impact of the COVID-19 epidemic on society [30], and how to control social activities to slow the spread of the virus [31]. For the COVID-19 disease, the conclusions reflected in social media data can help the government quickly understand the changes in people's daily behavior and the impact of government policies.

In terms of geographic information analysis, the geographic location information attached to social media data has become the most popular research object. Combining POI data and map information, researchers can analyze natural events [32], disaster management [33], and historical information [34] in a specific area from the perspective of big data [35]. The GNN model achieved better performance on the featured trend between tiles and can understand the location features in the geographic environment through training [13]. In geographic information analysis, both POI data and social data are unstructured text labels, and the graph structure with attention can complete the dynamics of the block features [36]. In order to analyze social data with time to geographic spatial movement, a spatio-temporal graph attention network is proposed [37]. This method is conducive to the change of text features on map tiles over time and im-

proves the ability of labels to describe the spatial features of the tiles. In this article, we use the spatio-temporal attention network for feature description and competitiveness analysis between map tiles of different categories.

The affection of COVID-19 with government measures is based on the popularity of social media services that enable the public to share their daily activities online. The geographic coordinates attached to some messages on social media can effectively collect user interactions in different scenarios at fixed locations. The content shared by users on social media can be used to describe the characteristics of places visited. This can help researchers to understand the dynamic trends in a specific area. The places on the map such as residential areas, schools, commercial areas, public squares, and transportation hubs are easy to divide into fixed areas with city facilities and functions. The dynamic change of user access from social media data reflects the user's preference of city facilities on the map, and the relation of different user visits in the same category of city facilities can be called competitive relationship. In previous research, the places visited attributes are collected from POI data and contribute to investigating a unique perspective for understanding the competitive environment by measuring the competition between POIs. The study of competitive relationship prediction has been a hot research topic for a long time. Most of the existing works aim at solving the competition prediction between social events, companies or products. A new POI competitive raster prediction model is proposed, which aims to identify the dynamic degree of competition between map raster units and urban facilities. In this thesis, the regional competitiveness on the map will be introduced to describe the attributes that are different from the dynamic label assigned in the map raster process.

3 Problems and Solutions

Analyzing Diabetics for Food Access Training on the Map with CBAM

– Xie, Huaze, et al.

Chapter Contents

3.1	Chapter Overview	17
3.2	Problems	17
3.3	Map Tile Selection	18
3.4	Map Rasterization	18
3.5	MRSS	20
3.6	Comparative Experiment	22
3.7	Result	23
3.8	Conclusion and Discussion	24

3.1 Chapter Overview

In this chapter, a review of the problems in this thesis and the solutions of the basic works will be introduced. In addition, a set of comparative experiments will be proposed to extract the map tile for rasterization and improve the training efficiency.

3.2 Problems

This thesis focus on the problem of:

a. Data selection for which kind of input format?

In this thesis, data base is collected from the Google base map, POIs are collected from Open Street Map, and social media data is collected from Twitter short text with geolocation information.

b. How to describe short text data map to the POIs?

The short texts from Tweets are normalized with graph structures. Each node in graph structures is a Tweet and connected with related POIs by edge information.

c. How to define the map zooming process and zoom level?

The zoom levels from visualization, are represented as base map: $z = 0$, visual zoom levels: $z = 1, 2, 3$.

d. After graph training, how to focus on the interest POI categories?

A global attention mechanism will be used for the training process is focused on the related POI categories.

e. How to train the raster competitiveness?

For raster competitiveness, a new framework: RC-GAT is proposed to train the user preference and trend of user's behaviors with related POI categories.

3.3 Map Tile Selection

In Figure 2.3, introduces **the process of cell feature extraction on the rasterized map tile**. The traditional geographic information is usually constructed by the vector model, and the vector data includes geometric figures (points, polylines, polygons) to represent the real world.

Figure 2.3 describes **how the vector data of POIs from the Google Maps API composed the process of priori map tile datasets**. The left is an ordinary map from OpenStreetMap. In the middle map, the spatial vector information, building attributes, placemark attributes, and feature information of the area are imported to the base map and three map tiles with roads are cut in the red circle. Finally, three tiles (tile: A, B, C) are derived with a priori features, which contain the main feature of the shopping area and restaurant (Map Tile: A), the main feature of travel attractions and souvenir shopping area (Map Tile: B), and the main feature of another shopping area (Map Tile: C). In this study, the map areas with dense POI marks or crowded social media data with geolocation will be segmented into discrete map tiles by roads as the underlying research dataset.

3.4 Map Rasterization

Raster maps use a pixel matrix to represent the base map, and each pixel contains a value to describe the hidden condition of the area covered by the pixel.

In this thesis, the classic map tile rasterization is utilized to display the information that is continuous across regions and cannot be easily divided into vector features. Through software such as QGIS, the geographical information in Google Maps is converted into basic raster data such as the process in Figure 3.1. The base feature map contains the cell value of each raster unit. In the next process, a 2×2 max pooling layer is the convolution of raster feature information of the area are imported to the base map and summary the map tiles with roads are cut in the red circle. At last, a new feature map represents the map feature of map tiles.

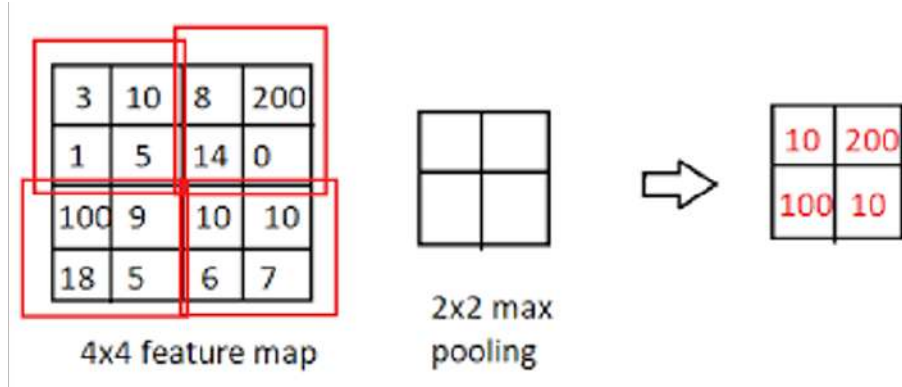


Figure 3.1: An example of rasterized map tile with feature map extraction process.

In addition, **the POI attributes are expressed into 5-dimensional features** including restaurants, hotels, transportation, travel attractions, and shops. This is conducive to the coverage density in map spatial information and helps our node feature summary of the priori data set in this paper. A 130 priori map tile dataset with POI and social media data is produced of 50×50 meters standard rasterized units.

Social media data from Twitter is divided into 5 POI categories and mapped to the POI in each raster unit, where the 5 POI categories are denoted by \hat{A} ($\hat{A} \in A_1, A_2, A_3, A_4, A_5$). The POI category of each user post-Tweet $Tweet(P)$ is

$$Tweet(P) = \sum_0^i \hat{A} * i(positive) \quad (3.1)$$

where i is the number of Tweets and only "positive" Tweets matching the POI category is credited to the corresponding POI attribute. Each Tweet contributes POI category \hat{A} as an augmented vector shown in Figure 3.1. Combined with the POI and Tweet geolocation, each POI related positive Tweet position is denoted in each raster unit $R_{p_{\hat{A}}}$

$$R_{p_{\hat{A}}} = \sum_0^n Tweet(P) * n(Lat, Lng) \quad (3.2)$$

where n is the raster unit number of each Tweet's position, and (Lat, Lng) is the coordinate of the Tweets. After importing the social media data into the map tile, the POI graph structure G_M is constructed on the map tile.

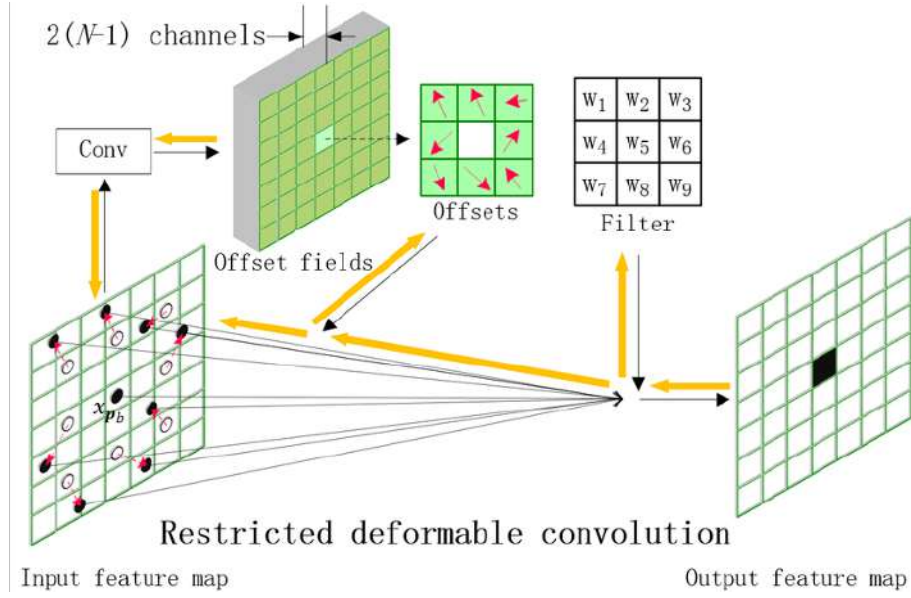


Figure 3.2: The process of raster unit convolution and cell feature extraction.

3.5 MRSS

For raster map tile training, has a difference between **traditional convolutional image (Euclidean Space)** and **graph (Non-Euclidean Space)**. In the Euclidean Space represented by the image, the node-neighbor has a definite number, and the convolution operation uses a fixed-size learnable convolution kernel to extract pixel features. But in a non-Euclidean Space of the graph, the number of node-neighbor is not fixed, and the traditional convolution kernel cannot be used to extract the features of the nodes.

For **graph convolution networks (GCN)**, the realization of convolution using graph Fourier transform like spectral convolution. It means the Laplacian operator in the spectral-domain is derived by using the Laplacian matrix of a graph. The formula of graph convolution is derived by analogy with convolution in Euclidean space in the spectral-domain. For a graph $G = (V, E, W)$, V is a finite set of $|V| = n$ nodes, E is a set of edges among nodes and $W \in \mathbb{R}^{n \times n}$ is a weighted adjacency matrix representing the weights of edges. An input vector $x \in \mathbb{R}^n$ is seen as a signal defined on G with x_i denotes the spectral information of node i shown in Figure 3.2.

For the **spectral-domain convolution of an undirected graph**, the relationship between the feature function f and the convolution kernel g can be expressed as follows:

$$(f * g) = F^{-1}[F[f] \odot F[g]] \quad (3.3)$$

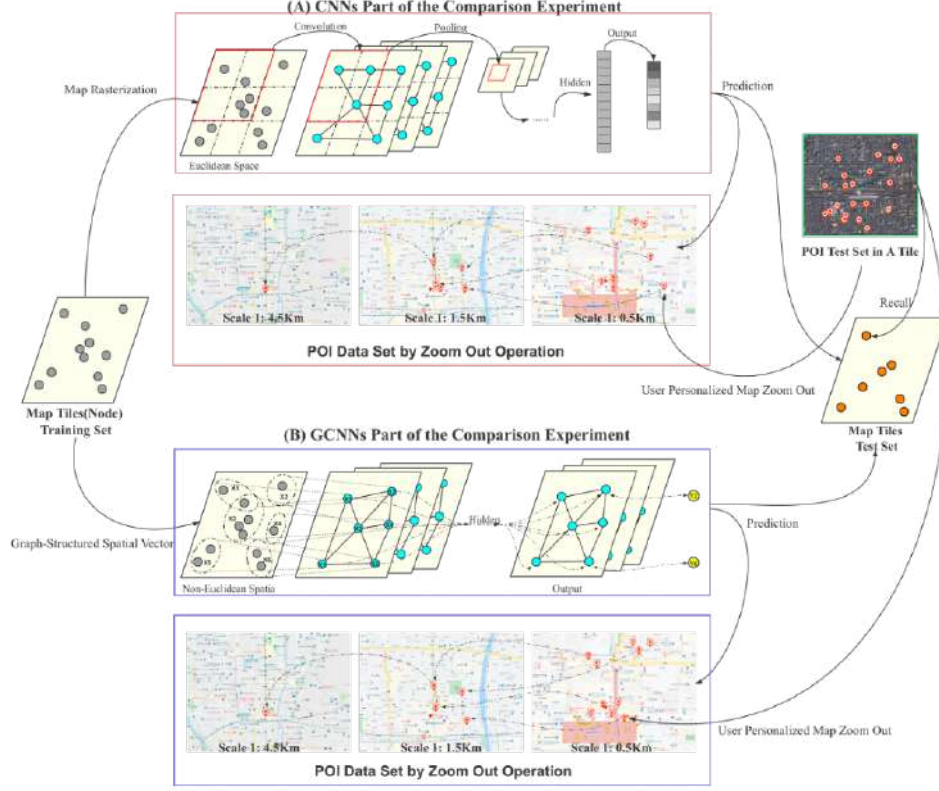


Figure 3.3: The comparative experiment with CNN (A) and GCN (B) training process.

$$(f * G_g) = U (U^T f \odot U^T g) = U (U^T g \odot U^T f) \quad (3.4)$$

Put the $U^T g$ as a learnable kernel write as g_θ , the final convolution formula is:

$$o = (f *_{G} g)_{\theta} = U g_{\theta} U^T f \quad (3.5)$$

Suppose the hidden state of layer l is $h^l \in R^{N \times dl}$, the status of the spectral-domain convolutional layer is updated to [38]:

$$h_{ij}^{l+1} = \sigma \left(U \sum_{i=1}^{d_l} \Theta_{ij}^l U^T h_{ij}^l \right) \quad (3.6)$$

So far, the basic theories is briefly introduced and will be used in the next comparison experiment between CNN and GCN.

3.6 Comparative Experiment

In order to satisfy the CNN and GCN training models with the feature information in the map tiles, **the rasterized tiles solve the Euclidean Space problem** proposed in Figure 3.3. By rasterizing map attributes, the priori tile training set input to the CNN and GCN models for training. In addition, training models are normalized to unify the predictive ability of the model. For CNN, in the case of one-dimensional time series data, the model can be characterized as:

$$y_i = \sum_{j=0}^{L-1} W_j x_{i+j-\frac{L}{2}} \quad (3.7)$$

where L is the length of convolution kernel, $W_j \in \mathbb{R}^{\text{fout} \times \text{fin}}$, and $y_i \in \mathbb{R}^{\text{fout} \times 1}$. The definition of $g_j \left(x_{i+j-\frac{L}{2}} \right) = W_j x_{i+j-\frac{L}{2}}$, from Eq. (3.7):

$$y_i = \sum_{j=0}^{L-1} g_j \left(x_{i+j-\frac{L}{2}} \right) \quad (3.8)$$

For GCN, a generic non-local operation can be defined as [39]:

$$y_i = \frac{1}{C(x)} \sum_{\forall j} f(x_i, x_j) g(x_j) \quad (3.9)$$

where $x_i \in \mathbb{R}^{\text{fin} \times 1}$, is the feature of node i . $f(x_i, x_j) \in \mathbb{R}^0$ measures the similarity between two nodes, and x_i, x_j are defined by the edge between nodes or not.

Compare with the Eq. (3.8) and Eq. (3.9), both CNN and GCN will perform spatial transformation on node: $g_j \left(x_{i+j-\frac{L}{2}} \right)$ and $g(x_j)$. In the CNN model, different nodes have different spatial transformations. In the GCN model, the spatial transformation of each node is the same. So, the spatial transformations are summarized as not shared with different nodes [40]:

$$y_i = \frac{1}{C(x)} \sum_{\forall j} f(x_i, x_j) g_j(x_j) \quad (3.10)$$

Figure 3.3 introduces the process of comparative experiment, contains a priori map attribute data import in the CNN and GCN, and normalized prediction of the two methods.

Table 3.1: The Prediction Results of Comparative Experiment Between CNN and GCN Models

	MAPE (30 Tiles)		MAPE (60 Tiles)		ROC		PRC		POI Recall	
	CNN	GCN	CNN	GCN	CNN	GCN	CNN	GCN	CNN	GCN
Restaurant	27.851%	24.540%	27.982%	24.371%	0.767	0.797	0.053	0.163	0.735	0.792
Hotel	55.516%	49.765%	54.904%	49.632%	0.758	0.742	0.062	0.117	0.752	0.782
Transportation	35.246%	39.439%	38.668%	38.510%	0.742	0.753	0.060	0.136	0.803	0.785
Travel Attraction	43.395%	36.086%	43.382%	35.755%	0.739	0.755	0.057	0.145	0.734	0.781
Shop	34.296%	28.911%	34.720%	28.417%	0.753	0.794	0.055	0.148	0.753	0.826
Average	39.261%	35.748%	39.931%	35.337%	0.7518	0.7682	0.0574	0.1418	0.7554	0.7932

3.7 Result

In this chapter, **160 map tiles of Kyoto City are used to complete the map attribute labeling** including restaurants, hotels, tourist attractions, transportation, and shops through Google Maps API. In Figure 3.3, **a set of comparative experiments are completed with CNN and GCN**, and the predictive evaluation index: Mean Absolute Percentage Error (MAPE) is used to describe the continuous prediction results. In Table 3.1, the performance of CNN and GCN in two data sets are listed with the 30 and 60 test tiles, and also introduce the ability of two models the processing POIs regression data.

In Figure 3.3, a set of comparative experiments are completed with CNN and GCN training model. According to the evaluation index MAPE (while a MAPE value of 0% indicates the best model and a MAPE value greater than 100% indicates an inferior model), the prediction results are performed in Table 3.1. The transportation attribute of the MAPE result in the CNN model is 35.246% better than the result of 39.439% of the GCN model. The prediction results with the other four attributes as the target of testing, GCN obtain the MAPE results (24.540%, 49.765%, 36.089%, and 28.911%) better than the CNN results (27.851%, 55.516%, 43.395%, and 34.296%).

In another set of 30 comparison test map tiles, the MAPE prediction of Restaurant is 27.951% (CNN) and 24.540% (GCN), and in a double-size data set, the MAPE is 27.982% (CNN, increase) and 24.371% (GCN, reduce). And for attribute: Transportation, the MAPE of 30 tiles is 35.246% (CNN) and 39.439% (GCN), and the MAPE of 60 tiles is 38.668% (CNN, increase) and 38.510% (GCN, reduce).

From Table 3.1, both CNN and GCN models complete the task of classifying place-mark attributes from map tiles. POI Recall is used to describe the performance of the POI in the prediction result. The results show that compared to the CNN and GCN model has more advantages in the classification task combine with placemark attribute tiles based on raster statistics units. And **the GCN model is better to describe the**

POI in the process of map zooming with more personal information.

3.8 Conclusion and Discussion

This chapter introduces **a statistical method of map attribute rasterization: MRSS**. By rasterizing the spatial information and feature information of 100 map tiles in Kyoto City, another 60 tiles are used to predict tasks in two datasets. For 160 priori tiles feature data set, **a set of comparative experiments designed with CNN and GCN models by analyzing the raster attributes** including tourist attractions, restaurants, hotels, transportation, and shops. In this test, **the local relationship feature filter is used to adjust the training models' ability to understand the features of priori tile datasets**. Compared with the CNN model, the advantages of the GCN model are:

1. The GCN model has more advantages in judging the regression distribution of placemark features after the map zoomed by the distance between the training sampling locations, which also shows that the GCN model is more suitable for the user's map preference.
2. The GCN model can connect the feature nodes corresponding to all raster attributes, and has a stronger ability to learn a priori map tile data.
3. The training can be completed by importing the features of the entire map tiles and easy to understand the associated features between the tiles.

In this chapter, the dataset which is contributed come from a set of priori training sets, and the problem is that without using a priori map feature data set, the CNN or GCN model cannot learn the POI attributes in the map and cannot predict the map tile features.

Part II

Applications

4 Application I: Map Zooming Processing

*A GNN Map Tiles Extraction Method Considering POIs
Priority Visualization on Web Map Zoom Dimension*

– Xie, Huaze, et al.

Chapter Contents

4.1	Chapter Overview	27
4.2	Background	28
4.3	Data Collection	29
4.4	Raster Processing	30
4.5	Framework: SZ-GAT	31
4.5.1	Process Overview	31
4.5.2	MRSS for Zooming	32
4.5.3	Graph Structure	33
4.5.4	Global Attention Mechanism	34
4.5.5	Map Zooming Process	35
4.6	Evaluation and Experiment	36
4.6.1	Settings	36
4.6.2	Dataset	37
4.6.3	Baselines	37
4.6.4	Evaluation Results	39
4.6.5	Case Study	40
4.7	Conclusion and Discussion	41

4.1 Chapter Overview

In this chapter, an application of the MRSS framework will be introduced with the collected Kyoto POI data and Tweets. In this application of MRSS, motivated by the problem of the dynamic POI attributes analysis at multiple map scales, **a spatial-zoom graph-attention model (SZ-GAT)** is proposed with a global-attention mechanism and 5-category POI attributes at each raster zoom level. Furthermore, **a social-media dataset (Twitter with geolocation)** will be utilized to promote POI visualization at different zoom levels and improve the aggregation efficiency of geographic records in zoom dimensions.

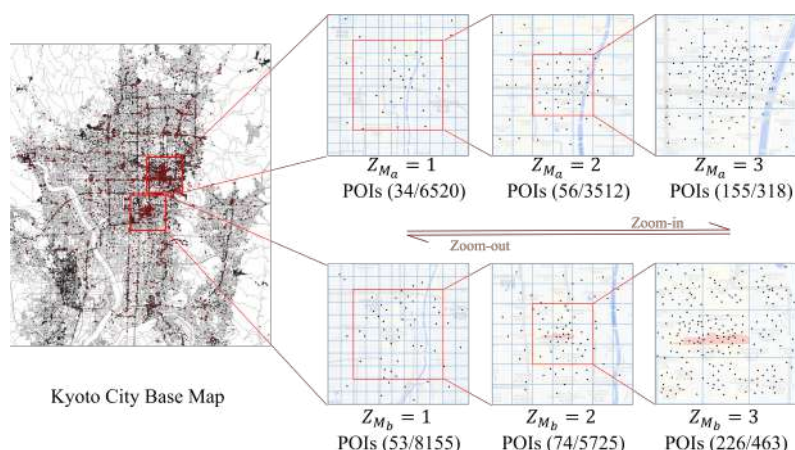


Figure 4.1: The detail of POI within map zooming on the example of Kyoto Base Map where the map zooming level: $z = 1$ (1:100000), $z = 2$ (1:10000), $z = 3$ (1:1000).

This application aims to extract the POI geo-features from Twitter and display the user's favorite POI category at three map zooming levels. The evaluation of the POI prediction results is based on the Google, OpenStreetMap, Bing, and Yahoo! web map platforms by comparing the category of user visit history on Twitter (including restaurants, hotels, transportation, etc.)

4.2 Background

Owing to the increasing popularity of social media services, mobile terminals have enabled the public to share their daily activities online and leave their digital footprint in urban areas. The information provided by social media reflects the real-time characteristics (flows, services, scenery, and parking) of urban facilities such as restaurants, transportation, and attractions. GPS coordinates within urban areas collected by geotagged social-media messages help researchers understand dynamic spatially oriented human activities and spatial urban patterns. For the web map, the zoom-in and zoom-out operations easily observe every country, city, and street. Displayed categories (buildings, placemarks, streets, and boundaries) gradually increase when the map zooms in and disappear when it zooms out such as the process of Figure 4.1.

The geographic characteristics displayed from a country to a street-level scale are called the LOD on a map. Particularly, the web map is composed of several tiles, and each map tile displays only a small part of the placemark names and hides most of the geographic information. The dynamic characteristics of map tiles are described by POI data, where the location based on users' visit history records are the underlying pattern of trips and spatial interactions in cities, POI revisited-spatial interaction, and distance

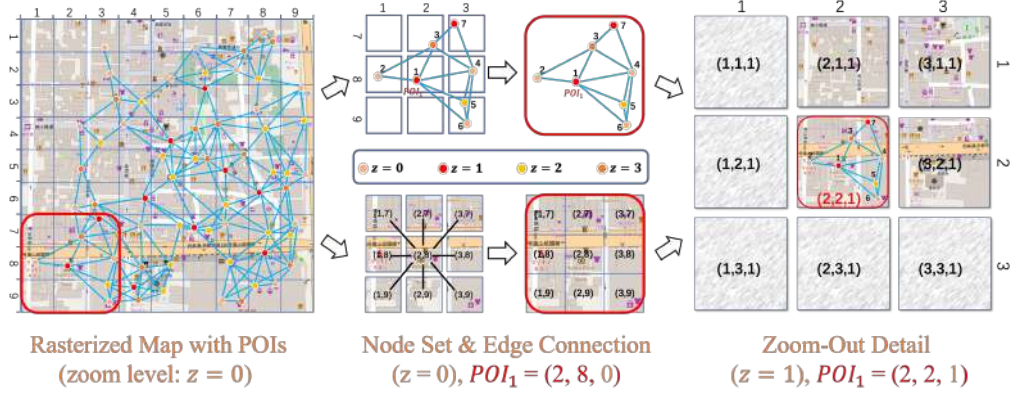


Figure 4.2: A Google base map tile with POIs zooming process in zoom level 1 and the detail of rasterized tile units zoom-out segmentation.

decay in spatially embedded networks. **In this application, the problem of users' favorite POIs at multiple map zooming level visualization and POI dynamic display (zoom-in) and disappearance (zoom-out) on the map will be solved by the SZ-GAT framework.**

4.3 Data Collection

In this application, the collected data included location information and map-tile data. **Location information** is a set of POIs with geographical information used to describe the dynamic changes in the map-zooming process. The collection of POIs is tiered according to the zoom levels shown in Figure 4.2, which all the POIs are displayed on the base map in zoom level 0. The **map-tile data** are a set of vector maps containing dense POI cores from different map platforms, as shown in Figure 4.3. The map features were collected from the Google Map API as follows:

1. **Base map:** from Google Road Map in the area, used to visualize the division of map tiles;
2. **POIs:** from OpenStreetMap, utilized to determine the scope of the basic POI data set in the area;
3. **Placemarks:** from Google-map-location reviews and Foursquare, used to count the popularity and user behavior of each placemark;
4. **Tweets with geolocation:** used to evaluate the user visits and preferences in the map-zooming process of the proposed model.

The dense POI cores are divided into 160 maps using roads for rasterized map feature extraction as shown in Figure 4.2. In order to classify each POI as a trainable POI attribute on the base map more efficiently, we focus on 5 kinds of POI categories. In



Figure 4.3: An example of POIs and Tweets with geolocation on the Google Base Map, where the POIs and Tweets are divided into 5-dimensional categories to provide the trainable POI attribute vectors.

Figure 4.3, the rich POIs and Tweets with geolocation are extracted on the Google Base Map, where all the POIs and Tweets are divided into 5-dimensional categories including restaurants, shops (convenience stores, markets, and malls), transportation (parking, stations, and airports), travel attractions, and hotels. **The Tweets are the user visit history utilized to contribute the POI-related attributes**, such as the Tweet "2147483647," which provides the POI "genzo" attribute restaurant as A_1 . The five POI categories correspond to the five trainable POI attributes $A_1, A_2, ..., A_5$. Google map reviews and Foursquare data were initially used to label the POI categories.

The POI dynamic change are introduced at the three zoom levels shown in Figure 4.1. One-month Tweets were imported as red marks because they were affected by the resolution and layout of the map. The display of POIs results from different platforms: OpenStreetMap, Bing Maps, and Yahoo! Maps with three zoom levels used to evaluate the training model results.

4.4 Raster Processing

Map tile raster process of SZ-GAT is improved from MRSS. **POIs and Tweets are represented with LOD through data generalization, and the dynamic POI display on different map scales is called map zooming.** The base-zooming attribute is defined using the coordinates and the zoom level. The zoom level with nine tiles are defined as a new map in the zoom-out process shown in Figure 4.2, where POIs are defined as different colors at different zoom levels. An example of POI1 in Figure 4.2 introduced the graph structure construction in which POIs are the node-set and adjacent unit connections are edge set. In this study, each raster-map-tile extraction contained the details of the POI attributes and zoom levels.

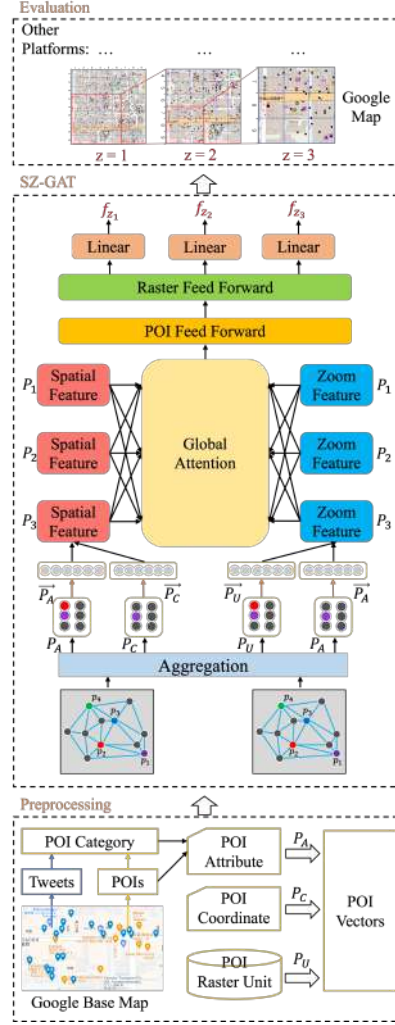


Figure 4.4: The overview of the SZ-GAT framework contains the Data Preprocessing Block, Map Tile Graph Attention Network Block, and Output Evaluation Block.

4.5 Framework: SZ-GAT

4.5.1 Process Overview

The visual information of the POI with the map zooming process could reflect the interest of the POI itself. This POI recommended method focuses on the dynamic changing with map zooming, just like the majority of user interest placemarks are displayed with map zoom-in. In this section, the zoom level of map tiles is used to discuss the related user interest features of POIs, in order to realize the map zooming visual function based on the location information and social media data. Figure 4.4 introduce the overview of the map zooming visualization with user preference process. The POI

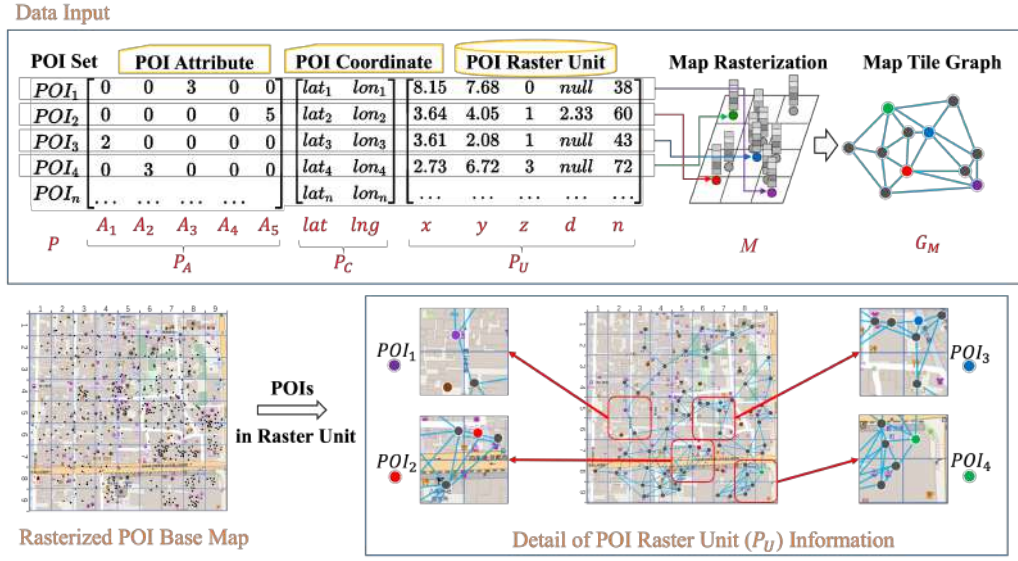


Figure 4.5: The detail of the input POI data set (Attributes, Coordinates, and Raster Unit Information), where A_1 to A_5 donate the POI location attributes in the category of Restaurant, Hotel, Transportation, Attraction, and Shop. lat, lng donates the latitude and longitude of the POIs. The map tile base features are donated by each raster unit's POI positions: flat position (x, y), zoom level: z , nearest POI distance d , and the number of the raster unit n in tiles.

features will be imported to different web map platforms including Google Map, Open-StreetMap, Bing Map, and Yahoo! Map. **The interest positions need to contain as few review redundant details as possible in order to reduce the cognitive load of processing raster units.**

Firstly, POI attributes with Tweets feature are mapped to the rasterized base map. Then, POI feature vectors are imported to the SZ-GAT training model, spatial and zooming feature of POIs visualize the user preference at three zoom levels. Finally, the POI prediction results with user preference on different web map platforms introduce our proposed SZ-GAT training model that works on different map zoom rules. Due to the map zoom rule of POI visualization in different map scales being different, the SZ-GAT training model is applied to train the POIs which contain 3 zoom levels of Open-StreetMap, Bing Map, and Yahoo! Map platforms.

4.5.2 MRSS for Zooming

The input POI attribute contains the POI attribute with Tweets, POI coordinates, and POI raster unit information and **the new vector of POI attributes contributes to the learnable graph structures**. G_M is a set of graph structure slices on the rasterized map tiles M , in which POIs compose the node set and the edges of the graph are fully

connected with the neighboring grid POIs, as shown in Figure 4.5.

Each user's post-tweet is mapped to the related POI category and combined with the POI information. The POI attribute P_A is defined as a 5-dimensional vector containing the features of restaurants, hotels, transportation, shops, and travel attractions. The output POI vector P contains the POI attributes P_A , POI position $P_C(Lat, Lng)$, and raster unit information P_U . P_C contains the geographical location (latitude and longitude) of each POI and user visit history. $P_U(x, y, z, d, n)$ is collected to describe the POI raster-unit information, where (x, y) is the position of the POI in the unit, z is the zoom level from 0 to z (example, $z = 0$: base map, $z = 1, 2, 3$: zoom level 1, 2, 3), d is the distance of the nearest-neighboring POI in the same unit, and n represents the POI's dynamic grid position in the map tile (for example, base map tile $z = 0$ has 81 units, and POI_1 position is on the 38th grid).

4.5.3 Graph Structure

The POI constructed graph of each raster unit $G = P, E$ comprises a placemark set P and a link set E within the grid. The vector of POIs is imported into the raster units, and the POIs are fully connected with neighboring grids to compose the graph structure G_p . For the rasterization map tile shown in Figure 4.5, M is denoted by a set of basic raster units $\{ M_{U1}, M_{U2}, M_{U3}, \text{ and } \dots, M_{Un} \}$. **Map tile is composed of a set of basic raster units in a 50 meters side square, raster unit is the basic POI statistics cell in a map tile, and these units represent the translation of the graph structure and map zooming.**

In the data preprocessing, we analyzed the tweets with 5 POI categories and mapped them to the POI in each raster unit, where the 5 POI categories are denoted by \hat{A} ($\hat{A} \in A_1, A_2, A_3, A_4, A_5$). The POI category of each user post-tweet $Tweet(P)$ is

$$Tweet(P) = \sum_0^i \hat{A} * i(positive) \quad (4.1)$$

where i is the number of tweets and only "positive" tweets matching the POI category are credited to the corresponding POI attribute. Each tweet contributes POI category \hat{A} as an augmented vector shown in Figure 4.3. Combined with the POI and Tweet geolocation, each POI related positive tweet position is denoted in each raster unit $R_{P_{\hat{A}}}$

$$R_{P_{\hat{A}}} = \sum_0^n Tweet(P) * n(Lat, Lng) \quad (4.2)$$

where n is the raster unit number of each tweet's position, and (Lat, Lng) is the coordi-

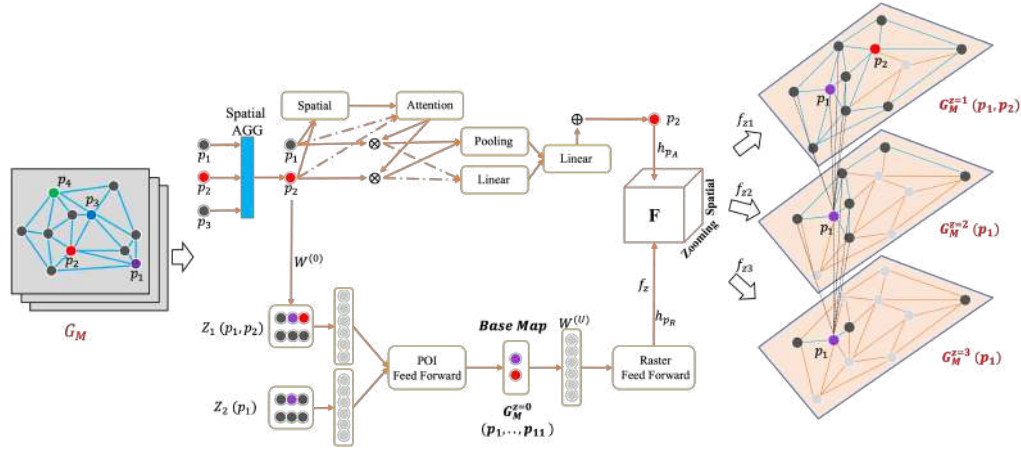


Figure 4.6: The process of our proposed method: SZ-GAT including Spatial Block and Zoom Block, the output layer shows the POI graph structures dynamic display in multiple zoom levels. (POI_2 is disappeared in zoom out process, $z = 2, z = 3$)

nate of the tweets. After importing the social media data into the map tile, we construct the POI graph structure G_M on the map tile, as shown in Figure 4.5.

4.5.4 Global Attention Mechanism

A fully connected POI graph structure on map tiles $G_p = P, E$. **The global attention mechanism is used to match the multilayer attention to the POI and focus on the 5-category attributes in the map-zooming process.** The graph attention network (GAT) [16] introduces a self-attention mechanism to learn the user-preferred visits of $P_{A_i} \in P \cup Tweet(P)$ to every POI node P . Each graph-attention-aggregation module updates the hidden H representations and aggregates information from every POI neighbor in proportion to the learnable attention coefficients. The aggregation operation of the l -th graph attention for placemark P in Figure 4.6 is

$$\vec{h}_P^l = \sigma \left(\sum_{i,j \in \{P_A\}} \alpha_{ij} \vec{h}_{P_0}^{l-1} W \right) \quad (4.3)$$

where \vec{h}_P^l is the POI feature embedding, σ is an activation function (ReLU), W is the trainable parameter matrix of the l -th layer, and α_{ij} denotes the attention coefficient between the placemarks P_i and P_j , which obey the following:

$$\alpha_{ij} = \text{softmax}_j \left(\text{attn} \left(\vec{h}_{P_i} W, \vec{h}_{P_j} W \right) \right) \quad (4.4)$$

where $attn$ is the attention mechanism, and $softmax$ is the regularized function of the selected node P_i neighbors.

The user visits POI feature h_P in each raster unit, which is simply described as follows:

$$h_P = \sum_{P_{A_1}}^{P_{A_5}} attn(Tweet(P_i)) W^{(0)} \quad (4.5)$$

On the Google base map of zoom level 0 in this application, all POIs with latitude and longitude are collected as coordinates. Figure 4.5 shows a 9×9 raster base map M . The grid contains the specific POI vectors h_P denotes the raster unit features h_R , and each POI position with the X-Y axis, zoom levels, the distance with the nearest POI neighbor in the same unit, and the number of units are recorded as a set of vectors h_{P_U} :

$$h_R = \sigma \left(\sum_{U_{P_i}} attn(h_{P_U}) W^{(0)} \right) \quad (4.6)$$

Same to the user visits POI feature h_P , each raster unit vector h_{P_U} contains a base map attention mechanism "attn" and the weight of POI attributes $W^{(0)}$ are shared in the same layers.

Tile feature F contains the POI attributes h_{P_A} , raster unit h_{P_U} shown in Figure 4.6 as follows:

$$F = \sigma \left(\sum_{f_{1,2,3}} attn(h_{P_U}, h_{P_A}) W^{(0)} \right) \quad (4.7)$$

where $f_{z(1,2,3)}$ denotes the POI prediction result features contained in each zoom level, respectively. **The output of POI features represent the user's preferences in each map tile.**

4.5.5 Map Zooming Process

Zoom Dimension is the visualization level of electronic maps in map tiles of different scales. In this section, "zooming" is exploited as a new flat map dimension, so that each POI can be drawn on the map tiles with an X-Y-Z axis. Five categories of map tile features are sequentially exported as the output of map zooming: zoom levels 1, 2, and 3. To describe the POI attributes contributed by 5-category tweet records in raster units. POIs are mapped to the linear zoom levels: $Z_{0,1,2,3} = exp(logZ)$, where $logZ$ is tiled linearly interpolated in the logarithmic domain as follows:

$$logZ = Z_0 + (Z_1 - Z_3) \times s/(s_1 - 1) \quad (4.8)$$

where s is the zoom step, s_1 is the step of the first zoom level, and $\log Z$ donates the linearly interpolate between map zoom level 3 and level 1, Z_0 is base map scales. P_A in spatial attention concatenate contains a POI 5-dimensional matrix R_A , and map feature h_M with zoom 3 levels includes a raster unit convolution process:

$$h^{M+1} = \sigma \left(\tilde{D}^{-\frac{1}{2}} \tilde{A} \tilde{D}^{-\frac{1}{2}} h^M W^{(U)} \right) \quad (4.9)$$

where $\tilde{A} = A + R_A^{z=1,2,3}$, $\tilde{D}^{-\frac{1}{2}} \tilde{A} \tilde{D}^{-\frac{1}{2}}$ is the normalized adjacency matrix of $G_M^z(p_1, p_2)$ in Figure 4.6, \tilde{D} is the degree matrix of \tilde{A} , and $W^{(U)}$ denotes the learnable parameter of map zooming unit levels.

Map tiles are zoomed as a new tile with next step of zoom dimension such as the red rectangle shown in Figure 4.2 comprises the units:

$$\begin{bmatrix} (1, 7) & (2, 7) & (3, 7) \\ (1, 8) & (2, 8) & (3, 8) \\ (1, 9) & (2, 9) & (3, 9) \end{bmatrix} \quad (4.10)$$

Zoom level $z = 0$ is ignored in the base map, and in the next stage, it was added to $(1, 7, 0)$. The position of POI_1 is $(2, 8, 0)$ in the zoom level 0 unit and $(2, 2, 1)$ in the zoom level 1 unit. To describe the unit features concisely, the position of each unit is rewritten as the count of the raster unit on the map tile. For example, unit $(2, 2, 1)$ is the 5th unit, and it is recorded as $n = 5$ in the 3×3 tile with zoom level 1 introduced in Figure 4.5. After the map tile zooms out to units $(2, 2, 1)$, POI_3 , POI_5 , and POI_6 disappear with map zooming, and the learnable parameter $W^{(U)}$ trains the POI features during the dynamic zooming of the raster unit.

4.6 Evaluation and Experiment

4.6.1 Settings

The SZ-GAT model is implemented using the PyTorch geometric platform. All POI positions were mapped to the 50×50 m grids of 160 map tiles by latitude and longitude. The zoom dimension of all map tiles is four levels ($z = 0$ for the base map, $z = 1, 2, 3$ for map zooming), the input POIs are 12-dimensional vectors, and the representation vectors are fixed to 108 dimensions. The cross-entropy loss utilized a batch size of one and ran the experiments for 100 epochs. We set the regularization coefficient to 0.001 and the initial learning rate to 0.001, followed by a decay of 0.0001 at the 10th epoch.

The slope in the LeakyRelu activation function was 0.2, weight coefficient was 0.4. We employed a fully connected neural network for POI-feature extraction from raster units, and the number of neurons in each layer corresponds to map-zooming levels of 225, 144, and 81. The threshold of the user favoring the POI number of each category with map zooming was set to 5.

4.6.2 Dataset

Tweets of user-visit-history datasets on the map tiles included three domains: spatial locations, visit attributes, and zoom dimensions. The real-world POI attributes P_A include five categories: restaurants, shops, transportation, hotels, and attractions, as shown in Figure 4.5, as A_1, A_2, A_3, A_4, A_5 . The domains of the labeled POI include the following:

- **Spatial Location:** learnable POI-placemark coordinates on a base map using the Google Map API: P_C as shown in Figure 4.5.
- **Visit Attributes:** the visit attributes are contributed by the social-media data of each POI. Google Maps was utilized to enhance the POI-visit attributes. Specifically, the tweet text usually provides unclear visit records, such as "Pudding" without geolocation. Therefore, we used Google-map reviews ("This restaurant sells pudding and sweet drinks.") to collect related POI-restaurant attributes.
- **Zoom Dimensions:** the raster-unit set P_U is collected by grid number n and zoom level z . The web-map-zooming dimension is visualized by three levels: $POI_1 : z = 1, 2, 3$ is POI_1 , shown on all three zoom-level maps in Figure 4.6. A threshold is given by a map zooming regular, in which the same attribute POIs in the same raster units compete on map zoom-out processing.

The dataset was divided into training, validation, and test sets. We collected 7,535,137 short texts with geolocation, of which 6,550,499 were Twitter data and 984,638 were from Google-Map reviews. Social-media data were mapped to the POI of each raster unit on the map tiles; 4,716,335 tweet records were utilized for a 100-tile training set, and 1,834,164 POI markers were recorded in a 60-tile test set. The remaining review set was used as the validation set.

4.6.3 Baselines

The proposed SZ-GAT model does not require completing the process of sampling the building in the fitting block with the sub-features, because a set of priority map tile data sets with POI spatial information is utilized to construct the graph structures.

The training groups contain a geographical distribution of tweet features on Google base maps and divided the dense POI core with roads as a set of trainable map tiles. Compare the SZ-GAT model with baselines, including a 3-dimensional dynamic graph convolutional network (3D-GCN), adaptive sequence partitioner with power-law attention (ASPPA), and graph-based geographical latent representation model (GGLR), and spatial-temporal-preference user dimensional graph attention network (STP-UDGAT).

- **3D-GCN [41]:** An GCN variant that model improved from DSTG and consider the POI visit preference on the 3D maps. The semi-supervised node-partition strategy on GCN provides the cross-pixel correlations.
- **ASPPA [42]:** ASPPA contains a stacked recurrent neural network framework Adaptive sequence Partitioner to identify the sequential patterns among semantic subsequences by automatically learning the latent structure in the user's check-in sequence.
- **GGLR [43]:** This is a graph-based POI recommendation model and considers the directed POI-POI graph constructed from check-in histories.
- **STP-UDGAT [44]:** This method focuses on the next POI recommendation task and the inclusion of user embeddings of global STP factors across all users to improve the recommendation task and user experience.

For the given POI test sample, for accuracy, if the shown POI is within the map zoom level D of the Google Base Map scale set, then a positive of 1 is awarded, else 0. The root means squared error (RMSE) and means absolute percentage error (MAPE) is used to evaluate the models.

$$RMSE = \sqrt{\frac{1}{n} \sum_{i=1}^n (a_i - f_i)^2} \quad (4.11)$$

The RMSE value represents the predicted value and the sample standard deviation of the residual between the predicted values. RMSE describes the sample discrete results. In this study, the nonlinear fitting training process, the smaller value of RMSE, the smaller dispersion between the prediction results of the training model and the actual value, and the model has better performance.

$$MAPE = \frac{100}{n} \sum_{i=1}^n \left| \frac{a_i - f_i}{a_i} \right| \quad (4.12)$$

The MAPE value of 0% indicates the best model and a MAPE value greater than 100% indicates an inferior model. The performance score is the recall of the test model POI attribute prediction as follows:

Table 4.1: The POIs Dynamic Zooming Display Prediction Result with 3D-GCN, ASPPA, GGLR, STP-UDGAT, and SZ-GAT training models.

Model		3D-GCN			ASPPA			GGLR			STP-UDGAT			SZ-GAT		
		Acc	RMSE	MAPE	Acc	RMSE	MAPE	Acc	RMSE	MAPE	Acc	RMSE	MAPE	Acc	RMSE	MAPE
Test Set A (30 Tiles)	level 1	51.33	25.71	39.18	43.17	28.33	40.05	55.25	24.16	39.53	53.16	24.73	38.11	58.72	22.95	35.25
	level 2	50.26	25.58	38.87	45.36	28.25	39.78	54.82	24.03	39.27	55.32	24.17	37.95	58.11	22.51	35.41
	level 3	50.55	25.53	38.62	46.08	27.96	39.47	54.96	23.58	39.55	55.58	23.49	37.62	59.04	20.36	35.28
	Average	50.71	25.61	38.89	44.87	28.18	39.77	55.01	23.92	39.45	54.69	24.13	37.89	58.62	21.94	35.37
Test Set B (60 Tiles)	level 1	51.77	36.88	41.69	45.18	39.61	43.27	55.85	36.04	42.63	55.70	36.65	41.05	59.15	34.85	37.18
	level 2	53.85	36.70	41.52	46.90	38.79	42.75	56.04	36.01	42.38	55.84	36.14	40.58	59.91	34.63	36.98
	level 3	54.20	36.58	40.96	48.73	38.50	42.05	56.28	35.86	40.96	56.47	35.28	40.17	61.08	34.06	36.72
	Average	53.27	36.72	41.39	46.94	38.97	42.69	56.06	35.97	41.99	56.00	36.02	40.60	60.05	34.51	36.96

Table 4.2: Users' preference POI score from dynamic zooming display prediction result with 3D-GCN, ASPPA, GGLR, STP-UDGAT, and SZ-GAT models.

Model		3D-GCN	ASPPA	GGLR	STP-UDGAT	SZ-GAT
Test Set A (30 Tiles)	level 1	64.35	61.56	64.22	71.37	84.52
	level 2	65.52	64.37	66.85	73.94	85.32
	level 3	66.39	63.50	66.14	69.15	83.85
Test Set B (60 Tiles)	level 1	61.27	61.48	62.92	70.33	83.55
	level 2	62.56	66.88	61.18	70.10	82.10
	level 3	62.73	64.91	63.24	71.04	83.61

$$Score = \frac{TP_{tweets}}{TP_{tweets} + FN_{reviews}} \times 100 \quad (4.13)$$

where TP_{tweets} is the positive tweet prediction and $FN_{reviews}$ is the negative prediction POI from Google-map reviews.

4.6.4 Evaluation Results

A randomly selected test set contains 60 map tiles and divides them into map tile sets A (30 tiles) and B (60 tiles), which contained five categories of user-visit POI attributes. The user-preferred POI is generated on the baseline method and SZ-GAT for three map zoom levels. The results are summarized in three tables. Table 4.1 introduces the prediction performance of each model, Table 4.2 shows the user-preference scores, and Table 4.3 shows the prediction accuracy for different web-map platforms.

Table 4.1 lists the performance of the 3D-GCN, ASPPA, GGLR, STP-UDGAT, and SZ-GAT models. Compared with the POI-processing ability of regression data of four models, the proposed method, SZ-GAT, outperformed the baseline models in user-visit regression and prediction accuracy at three zoom levels. Specifically, the average prediction accuracy of the raster unit in the 5-category attributes in set A improved from 44.87% of ASPPA to 58.62% of SZ-GAT. The RMSE performance is improved from 27.96%

Table 4.3: The Google map prediction result-based evaluation results of the OSM, Bing, and Yahoo! web map platforms.

Model		Google Map	OSM	Bing Map	Yahoo Map
Test Set A (30 Tiles)	level 1	58.72	58.57	54.61	55.06
	level 2	58.11	54.12	57.98	57.95
	level 3	59.04	53.62	57.85	58.64
Test Set B (60 Tiles)	level 1	59.15	58.40	56.04	56.29
	level 2	59.91	54.06	58.98	58.14
	level 3	61.08	55.35	58.37	58.16

of ASPPA to 20.36% of SZ-GAT in the test set A zoom level 3. The SZ-GAT achieved the best performance of 59.04% on the third zoom level of the Kyoto map. For set B, the results of the four training models were consistent with those of set A, where SZ-GAT obtained the best results from the average value. The RMSE and MAPE value show that the SZ-GAT has a good POI regression ability.

Table 4.2 compares with the user-preferred POI database from Google-Map reviews and lists the POI-performance scores of the test models that work on map tile zoom-out. The users' preference score improved from 64.37% to 85.32% for ASPPA and SZ-GAT in set A zoom-out map level 2. Compared with set A, the performance score reduced to 82.10% in set B zoom level 2 and obtained the best performance score of 83.61% in zoom level 3.

The results in Table 4.3 show the prediction accuracy of the POI mapping of the SZ-GAT model from the Google base map to OSM, Bing Map, and Yahoo! Map. Compared with the Google base map, the performance of OSM contained the best result of 58.57% and 58.40% in zoom level 1. In the second zoom level, Bing Map obtains the best performance of 57.98% and 58.98% in the test set A and B. For zoom level 3, Yahoo! Map has the best result of 58.64% in test set A, and Bing Map obtains the best performance of 58.37% in test set B.

4.6.5 Case Study

A case visualization of SZ-GAT prediction results is based on a Google Maps tile and evaluated with the Open Street Maps, Bing Maps, and Yahoo! Maps shown in Figure 4.7. Only POIs visited by more than 50 tweets are displayed on this map tile for map zooming visualization. POIs are divided into positive prediction results (orange dots), negative prediction results (green dots), and lost POI prediction results (blue dots). The prediction accuracy of the SZ-GAT training model is computed in three











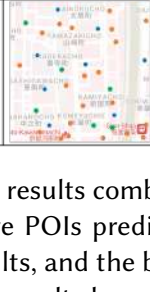

Model	Zoom Level 1		Zoom Level 2		Zoom Level 3	
a. Google Map	Error: 10 POIs: 25 Positive: 15 Acc: 60.00% Avg: 59.15%		Error: 12 POIs: 35 Positive: 22 Acc: 62.86% Avg: 59.91%		Error: 20 POIs: 60 Positive: 38 Acc: 63.33% Avg: 61.08%	
b. Open Street Map	Error: 12 POIs: 26 Positive: 15 Acc: 57.69% Avg: 58.40%		Error: 15 POIs: 36 Positive: 21 Acc: 58.33% Avg: 54.06%		Error: 25 POIs: 65 Positive: 40 Acc: 61.54% Avg: 55.35%	
c. Bing Map	Error: 11 POIs: 25 Positive: 14 Acc: 56.00% Avg: 56.04%		Error: 13 POIs: 34 Positive: 21 Acc: 61.76% Avg: 58.98%		Error: 23 POIs: 60 Positive: 37 Acc: 61.67% Avg: 58.37%	
d. Yahoo! Map	Error: 13 POIs: 27 Positive: 15 Acc: 55.56% Avg: 56.29%		Error: 12 POIs: 35 Positive: 21 Acc: 60.00% Avg: 58.14%		Error: 21 POIs: 58 Positive: 35 Acc: 60.34% Avg: 58.16%	

Figure 4.7: A case visualization of SZ-GAT prediction results combined with multiple web map zoom levels, where the orange marks are the positive POIs prediction of the SZ-GAT model, the green marks are the negative POIs prediction results, and the blue marks are the prediction results with lost POIs. The accuracy of the prediction results based on the Google Map test set is evaluated by the other web map platforms.

zoom levels of four web map platforms.

The proposed SZ-GAT model is derived from the zooming rules of Google Maps. Therefore, compared to the results of the other three web map platforms in Table 4.3, the performance of Google Maps obtains the best prediction results and has fewer losses of POIs after map zooming. Compared to the performance of the SZ-GAT model on the test set, the case of the map tile shows better performance at all zoom levels. The predicted results of this map tile case are better than the average of the test set. Considering the POI data composition of the case map tile, which aggregates a large number of business centers and tourist attractions and is one of the most tweet accessed areas in our tile set, we have reason to believe that **the performance of this case is an optimistic prediction and meets our training model expectations.**

4.7 Conclusion and Discussion

In this chapter, **a spatial-zoom graph-attention model is proposed to visualize the Tweet preference** with POI position features and retained map-tile-zooming characteristics using the raster statistics method. The user-visit-history data from Twitter and

Google Maps is adopted to enhance the POI attributes of each raster unit. The training of the proposed SZ-GAT model is completed and evaluated with other baseline methods. In the 160 pieces of a priori dense map tiles, **a set of user-access POI-zooming experiments is completed by analyzing 5-category POI attributes in the urban facilities.**

The evaluation results show that the prediction accuracy of test set B is slightly better than that of set A, as shown in Table 4.1. We examined the tweet attributes as test sets in different data sizes and found that the bigger the data size, the greater dispersion of the prediction result and the actual user-preferred POI data. We compared the category composition of the two test sets and found that Set A has numerous "Transportation" and "Restaurant," while Set B has 30% of "Attraction" in the POI-dense cores. Combined with the user-visit frequency, most of the attractions in Kyoto are temples with large areas. Therefore, the higher the frequency of visits to attractions, the more they can be expressed as users' favorite POI during the map-zooming process. **We believe that this is related to the user-preference map tiles with different urban facility functionality characteristics and that frequent user access is more representative of the attributes of this map tile.**

Compared with the baselines, the advantages of the proposed SZ-GAT model are as follows:

1. The SZ-GAT model has several advantages in terms of user-preference regression with tile zooming. The raster unit random sampling results show that the SZ-GAT model obtained better performance for tweet-attribute mapping.
2. The SZ-GAT model connected the POI features as nodes corresponding to all raster unit attributes and had a stronger ability to learn a priori map tile data.
3. The global attention mechanism focused on the given 5-category tweet attributes, POI attributes, raster unit features, and map-zooming results.
4. From the different test sizes, the performance of the SZ-GAT model was more stable, and as the test set increased, the prediction convergence of the SZ-GAT was better than that of the remaining baselines.

The experiments show that the SZ-GAT model achieved better performance than the baseline models. The SZ-GAT model matches the users' preference-related map tiles with different urban facility functionality characteristics. The map zooming dimension is a new field of map visualization and POI-data analysis. In future work, the SZ-GAT model will be applied to dynamic social data changing under the influence of social events.

5 Application II: Regional Competitiveness

*RC-GAT: Rasterized Competitiveness Graph Attention Network
for POI Visualization by Twitter Responses Since COVID-19*

– Xie, Huaze, et al.

Chapter Contents

5.1	Chapter Overview	43
5.2	Background	44
5.3	Framework: RC-GAT	45
5.3.1	Process Overview	45
5.3.2	Rasterized Competitiveness	45
5.3.3	Temporal Feature	47
5.4	Evaluation and Experiment	48
5.4.1	Settings	48
5.4.2	Dataset	49
5.4.3	Baselines	49
5.4.4	Evaluation Results	50
5.4.5	Visualization	53
5.5	Conclusion and Discussion	55

5.1 Chapter Overview

In this chapter, an application of the MRSS framework will be introduced with the collected Kyoto POI data and Tweets. A new word called regional competitiveness is used to define the user visit record in multiple placemark categories, which represents the access frequency of social data in each raster map unit to several attributes. In this application of MRSS, to reflect the dynamic changing in people's daily behavior with Japanese government measures since COVID-19, a **rasterized competitiveness graph-attention model (RC-GAT)** is proposed with a global-attention mechanism and 5-category POI attributes to predict the competitive place in different categories and map tiles as shown in Figure 5.1.

This application aims to extract the unstructured POI data and Tweets with geolocation records are mapped to the raster units. As the spread of COVID-19 disease and government anti-epidemic measures change the frequency of visits to the core of the city and the trend of regional competitiveness, the regional competitiveness

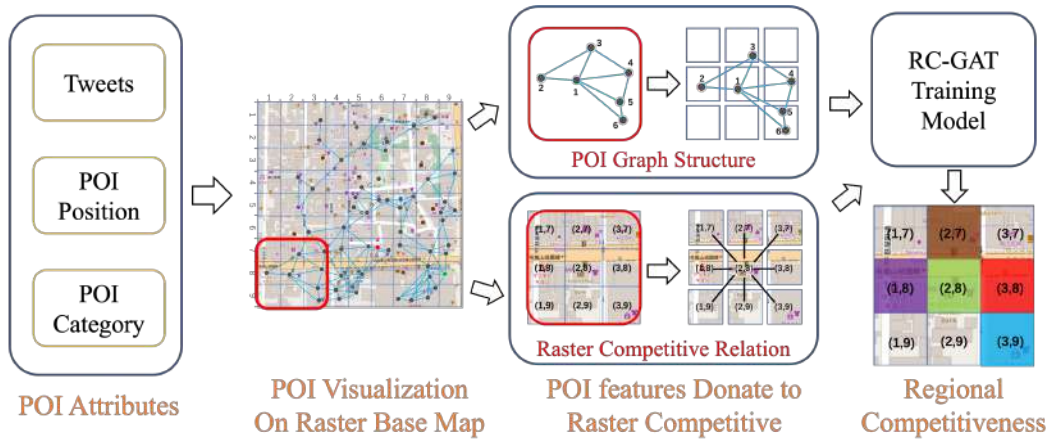


Figure 5.1: The overview of our proposed raster competitive relationship frameworks with the RC-GAT training model.

in the map tiles obtained by social media data and POI data visualizes the dynamic change analysis of crowd behavior activities and urban social functions.

5.2 Background

Since the outbreak of a new coronavirus disease: COVID-19 December 2019, this virus has spread all over the world [42]. According to the World Health Organization data, the first detected COVID-19 case in Japan was on January 20, 2020. With the spreading of the COVID-19 pandemic in Japan, the affected tourism industry also indirectly affects the revenue of the retail industry, restaurants, public transportation, and hotel service industries. For the retail industry and restaurants, the reduction in revenue comes from the cost of daily operations and includes the reduction in supply chain and demand [11].

A report from Economic Investigation Department introduced that after the Japanese government declared a state of emergency in response to the spread of COVID-19, consumption in one month was reduced to 43 about billion U.S. dollars. To make the COVID-19 spreading under control and minimize economic losses, the Japanese government has implemented a series of epidemic prevention and control measures and economic stimulus plans [1]. The Japanese government has formulated mitigation measures to slow the spread of COVID-19, but these measures have also directly affected the income of industries including retail, tourism, and public transportation. Correspondingly, the Japanese government adopted the "Go To Eat" and "Go To Travel" campaigns on October 1st, 2020, a business initiative designed to boost demand for industries that have been negatively impacted by COVID-19. In the dynamic environment with govern-

ment measures and people's consumption, we expect to introduce a method to describe consumers' consumption structure and trends in a fixed geographic area to observe the affection of government measures [2].

In this chapter, a rasterized competitiveness graph attention model (RC-GAT) is proposed that can efficiently extract POI geolocation features from social-media data and focus on the map tile dynamic attributes and competitive presentation. The Twitter data from January 1st, 2020, to December 31st, 2021, in Kyoto as social media data is collected in this application.

5.3 Framework: RC-GAT

5.3.1 Process Overview

In Figure 5.1, a POI visualized raster base map is used to describe our methodology and process overview. In the first place, the short text classification task is used to map tweets to 5 POI categories (restaurants, shops, hotels, transportation, and tourist attractions) in data preprocessing. Then, the Kyoto City map tile is divided into a set of meters grids, and POIs are imported to the map with geolocation and tweets information. Raster competitive relation and POI graph structure construction are introduced in this step. Finally, the rasterized competitiveness graph attention network is used to train the competitive relationship of POIs in 5-dimensional attributes in different scales of map tiles. For the competitive relationship visualization, we adopt 5 colors to display the dynamic changing of the raster unit's competitiveness, were brown for "restaurant", purple for "hotel", red for "transportation", green for "shop", and blue for "attractions".

5.3.2 Rasterized Competitiveness

After the Tweet data and POI data are imported to the base map by MRSS, the Tweet data will be mapped to the related POIs with 5 categories, the problem is that Tweet positions need to be aggregated with POIs on a raster unit. The common aggregation methods such as clustering are utilized for this type of map feature classification task [45]. However, the regional competitiveness should be trained as the evaluation criterion, the clustering method is difficult to cover and optimize the raster unit or map tiles to summarize the POI competitive relationships. We try to solve this problem with graph structure and introduce a graph neural network model (GNN) [46]. And adopt the attention mechanism with GNN to improve the aggregation efficiency of adjacent nodes and the correlation between Tweet data and POI data with graph structures [47].

Data Input

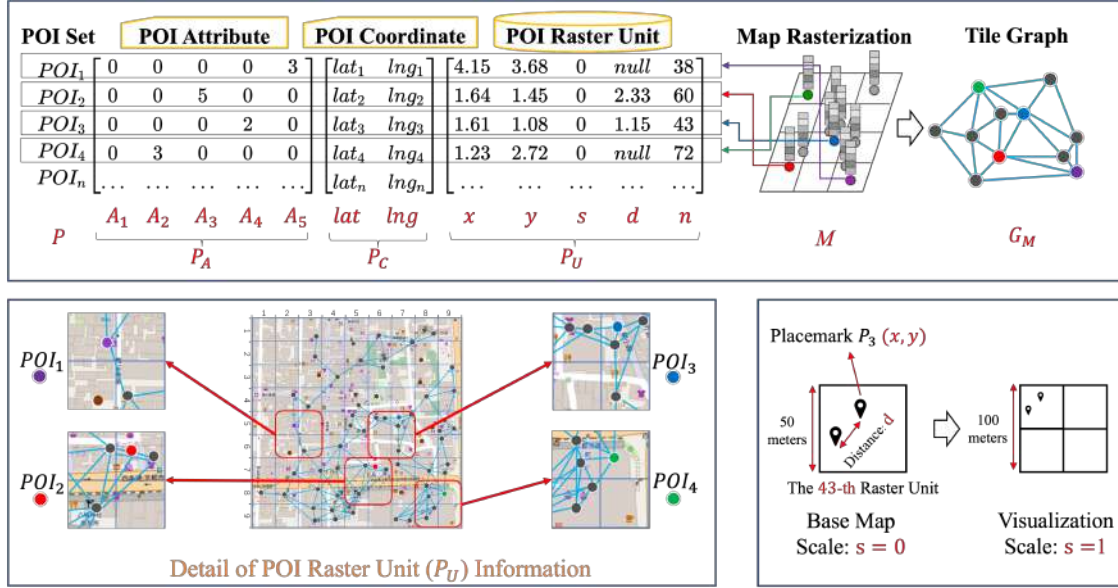


Figure 5.2: The detail of input POI data with P_A : POI attributes from Tweets in 5 categories, P_C : the coordinates of each POI, P_U : POI attributes of each raster unit.

In this subsection, the graph attention model (GAT) is utilized to analyze the 5-category POI competitive relation on the map tiles [48].

A graph G is used to describe the Tweets which are the users' visit history with geolocation as shown in Figure 5.3. The graph structure: $G_{Tweet} = (V, E)$, where V is the Tweet placemarks on the map as the node data, which summarizes the short Tweet records and coordinates. E describes the edge of the relation between Tweets and POI coordinates. To describe the POI feature combined with the learned short semantics, we first introduce the attention network of the queries to POI information which introduces the global relevance among queries and POIs. The global correlation between Tweet query: q and POI: p are denoted by the representation vector based on the general query to POI graph G_{Tweet} as [37]:

$$X_p = \sigma(a_{Tweet} * G_{Tweet} \times P_A W^0 + b) \quad (5.1)$$

where σ is the activation function, X_p is embedded Tweet queries on POI, W^0 denotes the weight matrices for Tweet position vectors, and b is the bias value. a_{Tweet} denotes the attention mechanism with graph G_{Tweet} . For a given edge: e combined with Tweets and POI categories, x_p is the POI node of embedded Tweets neighbours x_{Tweet} , we have:

$$a_{Tweet} = \frac{attn(x_p, x_{Tweet}, e, G_{Tweet})}{\sum_{V \in P(\hat{A})} attn(V, E, G_{Tweet})} \quad (5.2)$$

and the attention function defined as:

$$attn(P_{\hat{A}}) = LeakyRelu \left(W^0 \left(W^R \hat{A} \right) \right) \quad (5.3)$$

where W^R denotes the learnable weighted POI categories including: restaurant, shops, transportations, attractions and hotels on a raster unit. For any query to POI pair, the attributes of Tweets query and POI attention operation jointly determine the query to POI attention weight a_{ij}^P .

$$\alpha_{ij} = Softmax_j \left(attn \left(\vec{h}_{P_i} W, \vec{h}_{P_j} W^0 \right) \right) \quad (5.4)$$

where *softmax* is the regularized function of the selected node P_i and neighbor P_j . We define the map tile competitiveness *Comp* on the map scale s_1 with neighbor units *Comp*(u) aggregate:

$$Comp^{(s_1)} = \sum_{Comp(u)} \sum_{j \in N(i)} (L_{Tweets}(a_{ij}^P)) W^0 \quad (5.5)$$

Social media data from Twitter in Kyoto is used to specifically describe the regional competitiveness in the map tiles. A threshold is defined as if the same attribute denotes more than 5 pieces of the related Tweets in a single unit, the competitiveness of this unit will be visualized in the tile.

5.3.3 Temporal Feature

To visualize the dynamic competitiveness of rasterized maps, which requires that the output raster features contain time changes. A temporal description process T is adopted to the output feature F shown in Figure 5.3. The input raster feature h_{P_R} with monthly temporal competitive relation is:

$$h_{P_R} = \sigma \left(\sum_{R_i} \sum_{T=1}^{T=24} attn(Comp) W^R \right) \quad (5.6)$$

where T represents the temporal competitive feature *Comp*, and W is a global wight of map tiles. Tile feature F contains the raster feature h_{P_R} and map tile competitiveness

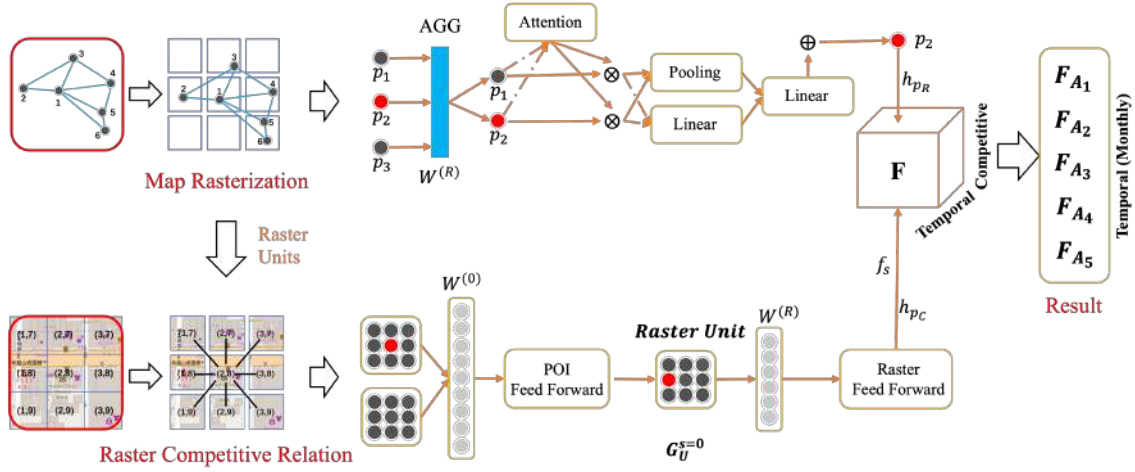


Figure 5.3: The process of the proposed RC-GAT framework. We input the POI graph structure and raster relationship to extract regional competitiveness and output the map tile feature in monthly 5 categories.

Comp shown in Figure 5.3 as follows:

$$F_{\hat{A}} = \sigma \left(\sum_{f_{1,2,3}} \text{attn}(h_{p_r}, \text{Comp}) W^R \right) \quad (5.7)$$

where $f_{s(1,2,3)}$ denotes the POI prediction result features contained in each zoom level, respectively. The output of POI features represents the user's preferences in each map tile.

5.4 Evaluation and Experiment

5.4.1 Settings

The RC-GAT model was implemented using the PyTorch geometric platform. All POI positions were mapped to the 50×50 meter grids of 100 map tiles by latitude and longitude. The visualization of the map scale is three levels ($s = 1$ for the base map, $s = 2, 3$ for result visualization), the input POIs are 12-dimensional vectors, and the representation vectors are fixed to 108 dimensions. The cross-entropy loss utilized a batch size of one and ran the experiments for 100 epochs. We set the regularization coefficient to 0.001 and the initial learning rate to 0.001, followed by a decay of 0.0001 at the 10th epoch. The slope in the LeakyRelu activation function was 0.2, weight coefficient was 0.4. We employed a fully connected neural network for POI-feature extraction from raster units, and the number of neurons in each layer corresponds to map scales of 225, 144, and 81.

The threshold of the user favoring the POI number of each category with visualization was set to 5.

5.4.2 Dataset

In this chapter, the dataset is collected from Tweets and user-visit-history on the map tiles, which included three domains: spatial location, temporal affection, and raster visualization. The real-world POI attributes P_A are denoted as five categories: restaurants, hotels, transportation, shops, and attractions from Twitter data, as shown in Figure 5.2, as A_1, A_2, A_3, A_4, A_5 . The domains of the labeled POI include the following:

- **Spatial Location:** learnable POI-placemark coordinates on a base map using the Google Map API: P_C as shown in Figure 5.2.
- **Temporal Affection:** the raster time attribute is contributed by the iterate monthly competitive relation. Specifically, we train the raster regional competitiveness from the monthly POI data set, and the raster unit features represent the competitive relation in different categories.
- **Raster Visualization:** the raster-unit set P_U is collected by grid number n and map scale s . We defined 3 dimensions of map scales $s = 1, 2, 3$ for the results visualization on the web map, where $s = 0$ is the raster unit with a side length of 50 meters on the base map. A threshold is given by the visualized category's regional competitiveness value in a raster unit that is greater than 10.

The dataset was divided into training, validation, and test sets. We collected 3,361,417 short texts with geolocation and mapped them to 100 Kyoto map tiles with POI. The training set is contributed by 2,835,184 Tweets on 80 tiles, and the test set is based on 526,233 Twitter records on 20 map tiles. The validation set is a set of POIs which are labeled by the Foursquare database.

5.4.3 Baselines

The proposed method does not require completing the process of the street or building feature sampling in the fitting raster, because a set of priori map tile data sets with POI location information is utilized to construct the graph structures. In the training groups, we considered the geographical distribution of Tweet features on Google base maps and divided the dense POI core with roads as a set of trainable map tiles. We compare our RC-GAT model with the baseline models including adaptive sequence partitioner with

power-law attention (ASPPA), graph-based geographical latent representation model (GGLR), and spatial-temporal graph attention network (ST-GAT).

- **ASPPA [42]:** ASPPA contains a stacked recurrent neural network framework adaptive sequence partitioner to identify the sequential patterns among semantic subsequences by automatically learning the latent structure in the user's check-in sequence.
- **GGLR [43]:** This is a graph-based POI recommendation model and considers the directed POI-POI graph constructed from check-in histories.
- **ST-GAT [44]:** This method focuses on the next POI recommendation task and the inclusion of user embedding with spatial-temporal factors across all users to improve the recommendation task and user experience.

To the given POI test sample, for accuracy, if the shown Tweet is within the basic raster unit P of the Google Base Map map tile, then a positive of 1 is awarded to the related POI feature, else 0. And we adopt the root mean squared error (RMSE) to evaluate the proposed model. The RMSE value represents the sample discrete results of POIs in a raster unit, which is a basic definition of regional competitiveness degree and reflects the training model predictive of discrete POI features. In general, for the nonlinear fitting training process of this paper, the smaller value of RMSE, the smaller dispersion between the prediction results of the training model and the actual value, and the model has better performance.

5.4.4 Evaluation Results

Social media data from Twitter in Kyoto is used to specifically describe the regional competitiveness in the map tiles. A threshold is defined as if the same attribute denotes more than 3 pieces of the related tweets in a single unit, the competitiveness of this unit will be visualized in the tile. As shown in Figure 5.4, all 5 attributes ("brown": restaurants, "green": shops, "red": transportation, "blue": tourist attractions, "purple": hotels) raster map tile of Kyoto Prefecture are utilized to describe the competitiveness of raster in $s = 3$ units in January 2020.

Figure 5.4 shows the geographical distributions of different raster categories with user preference results. The distribution of the cells corresponding to each category is relatively decentralized and mixed. To further explore the dynamic changing of each raster category, we used the road-divided Kyoto Map to reflect the user-visited urban

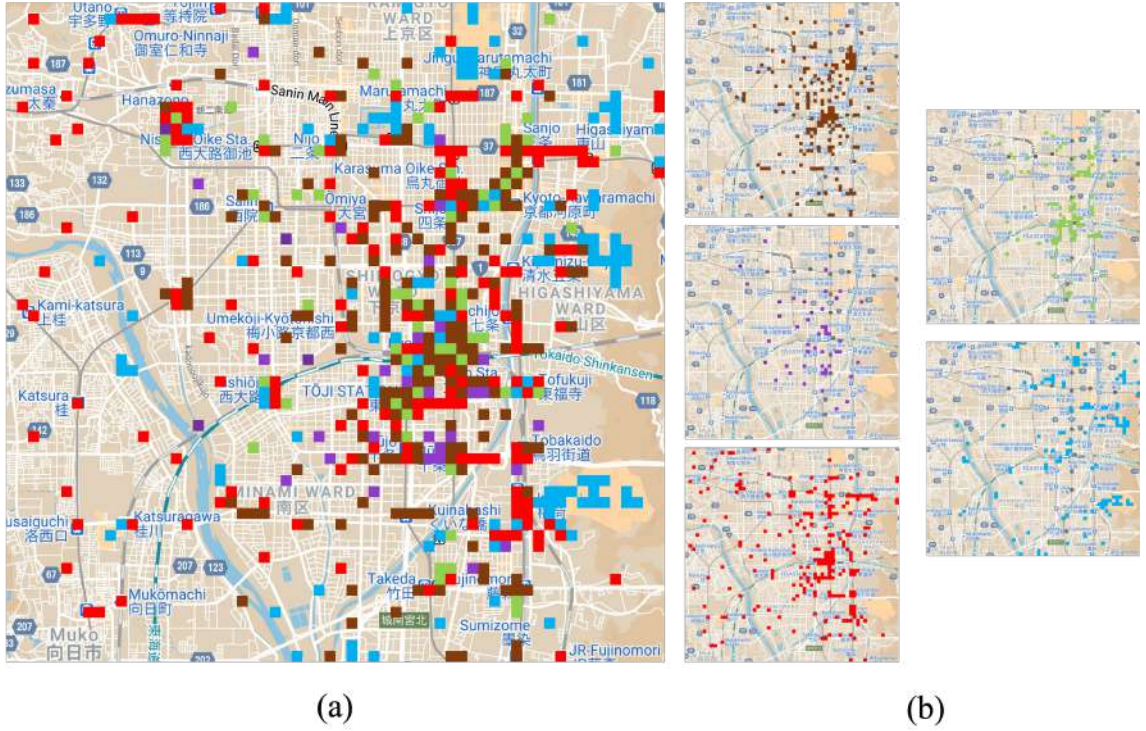


Figure 5.4: The result of raster competitive relation on the Kyoto City map in January 2020, where figure (a) is the overview of 5 categories, and figure (b) is the detail of "brown": restaurants, "purple": hotels, "red": transportation, "green": shops, "blue": tourist attractions, respectively.

core areas and the surrounding areas with social media data. We calculated the percentages of the raster unit in each category and compare the competitiveness of urban areas. The result shows the category: "Transportation" and "Restaurant" have a high percentage of 32.6%, and 26.4% respectively in Figure 5.4 (b). But the overall competitiveness shows in Figure 5.4 (a), the competitiveness of "Transportation" is 140.85, and the competitiveness of "Restaurants" is 72.6 in Table 5. **This means that in January 2020, users from social media were more competitive in their visits to the "Transportation" category.**

As shown in Figure 5.5, the dense core map tiles and the dense areas detail of Kyoto in 24 months reflect the spatial competitiveness of social media data and the dynamic process of user access on the timeline. In the case visualization of Kyoto Tower in Figure 5.5, we found that the tweet locations and geographic coordinates denote 5-category units. And the "shop" is more competitive in January means users are more inclined to go shopping in this area. Affected by the COVID-19 spreading, the unit's visit in April is less than the number of user visits in the previous three months. This map tile reflects the Kyoto government's intervention policy of restricting activities in April and May. **Compared with other months, the competitiveness of the "ho-**

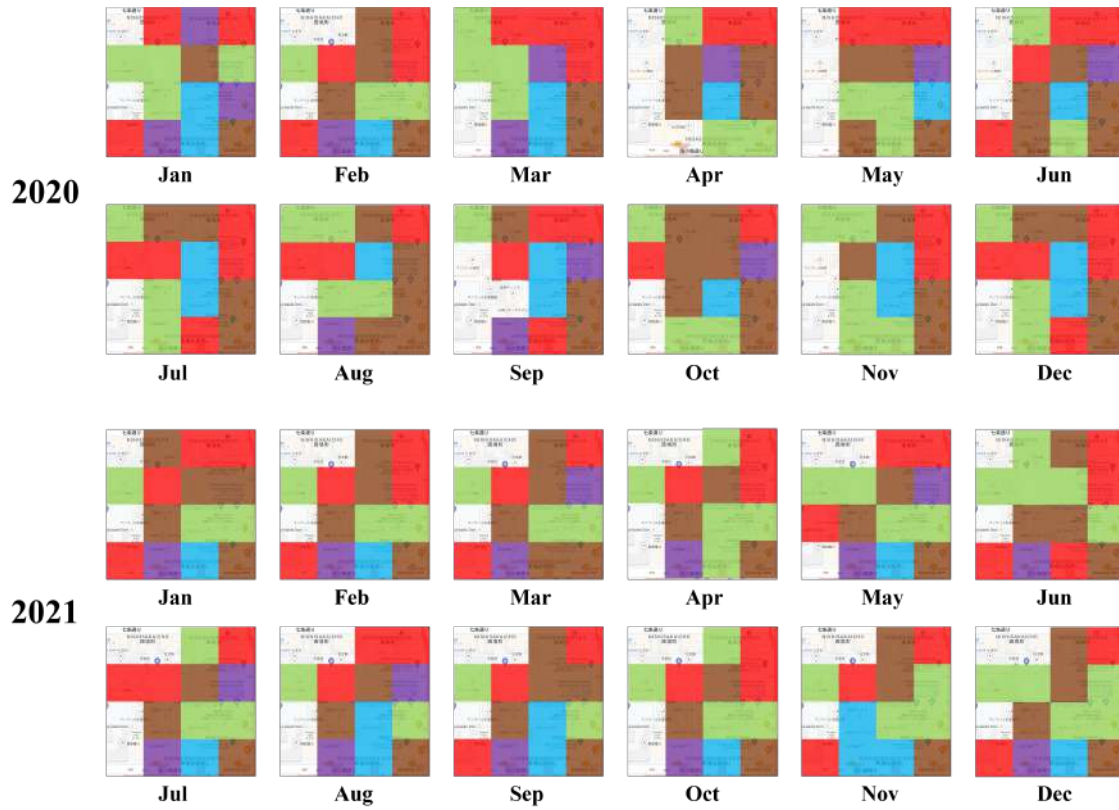


Figure 5.5: The case detail of the Kyoto Tower map tile dynamic changing in 24 months.

tel” category is declining, even disappearing in July and November 2020. There are fewer changes in the “restaurant”, “shop” and “transportation” categories, which represents the user’s visits are more inclined to eat, shop, and move on this map tile. We found that users’ needs for restaurants, shopping, and transportation are nearly not changed. And the utilization competitiveness of “hotel” and “attraction” categories are kept at a low level, this also explains the impact of tourist attractions and hotels during the spread of COVID-19.

We randomly selected 60 map tiles as the training set and 40 tiles as the test set from the 100 map set, which contained five categories of user access POI attributes. We generated the results of prediction accuracy and RMSE using the baselines and RC-GAT framework shown in Table 5.1. We list the performance of the ASPPA, GGLR, ST-GAT, and RC-GAT models and compared the POI-processing ability of regression data of four models, and evaluated them by RMSE. The proposed method, RC-GAT, outperformed the baseline models in user-visit regression and prediction accuracy in 5 POI categories.

Specifically, the prediction accuracy of the test set in the category of “restaurants” improved from 43.68% of ASPPA to 63.08% of RC-GAT in 2020 and 43.51% of ASPPA to 65.66% of RC-GAT in 2021. The RMSE performance is improved from 67.25% of ASPPA to

Table 5.1: The performance of the baseline training model: ASPPA, GGLR, ST-GAT and our proposed RC-GAT from January 2020 to December 2021.

Model(%)		ASPPA		GGLR		ST-GAT		RC-GAT	
		RMSE	Acc	RMSE	Acc	RMSE	Acc	RMSE	Acc
Restaurant	2020	67.25	43.68	46.33	53.16	31.68	59.64	27.06	63.08
	2021	65.94	43.51	45.91	54.55	31.25	60.19	26.49	65.66
Hotel	2020	58.73	46.35	43.07	57.49	30.24	61.37	26.4	68.42
	2021	58.26	48.04	43.22	57.61	29.88	61.81	26.33	69.03
Transportation	2020	75.06	39.9	52.65	50.36	43.57	58.32	31.35	65.01
	2021	73.55	40.16	51.69	50.24	42.13	58.64	31.06	64.57
Shop	2020	60.18	47.68	42.46	55.19	31.47	60.02	27.35	66.35
	2021	60.24	48.32	43.08	54.96	31.35	60.27	26.89	65.86
Attractions	2020	63.27	47.61	45.37	53.28	33.19	60.18	28.32	67.21
	2021	63.11	47.88	45.13	54.06	33.04	60.39	28.09	66.84
Overall POIs	2020	65.05	45.29	46.41	52.34	33.72	59.47	29.88	64.76
	2021	64.38	46.34	45.83	53.09	33.65	59.69	29.57	66.38

27.06% in 2020 and 65.94% of ASPPA to 26.49% of RC-GAT in 2021. RC-GAT framework achieved the best prediction performance of 69.03% and the best RMSE of 26.33% with the POI category of "hotel" on the Kyoto map. For the "transportation", "shop", and "tourist attraction" categories, the results of the four training models were consistent with "restaurants", where RC-GAT obtained the best results from the RMSE and prediction accuracy. **The RMSE value shows that the RC-GAT framework has a good regression ability of the residual between the predicted values and competitive related POIs.**

5.4.5 Visualization

In 2020, the response to COVID-19 spreading for the Japanese government included declaring a "state of emergency", and "preventing spreading" measures. A series of "economic stimulus" measures including the "Go To Travel Campaign" from July 2020 to February 2021, and the "Go To Eat Campaign" from October 2020 to January 2021 were launched to boost demand for industries that have been negatively impacted and to encourage people to travel and spend around Japan. In Table 5.2, the mark "↓" represents the government's intervention policy of restricting activities, the mark "*" denotes the measure of a single category, and the mark "↑" represents the economic promotion policy. Affected by the COVID-19 epidemic, in the map tiles of Kyoto Pre-

Table 5.2: The performance of RC-GAT framework regional competitiveness response of COVID-19 from January 2020 to December 2021 with government measures, where "↓" denotes the epidemic control measures, "*" is the unique measure to a category, "↑" represents the economic stimulus packages.

		Jan	Feb	Mar	Apr	May	Jun	Jul	Aug	Sep	Oct	Nov	Dec
Restaurant	2020	72.6	82.55	83.73	65.58↓	67.06↓	71.3	73.51	75.88	76.08	89.19↑	87.57↑	86.92↑
	2021	88.45↑	89.27↓	90.16↓	80.25*↓	65.73*↓	84.58*↓	83.26	59.44↓	56.71↓	77.35*↓	83.54	85.11
Hotel	2020	43.16	40.38	38.77	24.09↓	26.18↓	28.75	33.48↑	35.29↑	34.72↑	46.34↑	39.16↑	38.44↑
	2021	41.59↑	35.62↑↓	35.88↓	33.06	30.52	25.35	26.74	22.08↓	24.55↓	35.18	28.93	29.77
Transportation	2020	140.85	153.52	155.06	98.61↓	101.35↓	134.59	133.66↑	127.91↑	132.37↑	179.65↑	183.45↑	172.08↑
	2021	166.48↑	159.64↑↓	163.67↓	132.8	137.68	163.58	171.07	155.67↓	163.92↓	167.43	153.91	162.54
Shop	2020	86.19	83.27	85.38	62.08↓	60.75↓	78.46	79.11	77.34	78.66	80.13	80.42	79.68
	2021	81.06	73.58↓	74.05↓	77.35	79.83	81.49	80.22	76.54↓	75.6↓	79.28	83.52	81.49
Attractions	2020	51.93	53.45	52.84	35.16↓	33.24↓	45.28↑	44.9↑	40.29↑	39.84↑	43.28↑	49.07↑	48.5↑
	2021	46.35↑	42.17↑↓	42.32↓	45.48	52.33	49.64	50.15	45.82↓	43.09↓	51.74	48.66	53.62



Figure 5.6: The COVID-19 response sensitivity of Kyoto regional competitiveness based on the RC-GAT model with the data in Table 5.2.

Figure of Figure 5.6, the regional competitiveness contributed by social data indicates that the frequency of visits and competitiveness of "transportation" is the highest, and the competitiveness of "restaurants" follows government policies. The regional competitiveness of "shops" only follows the policy changes in 2020 and was not obviously affected by government policies in 2021. The changing of "Tourist attractions", and "hotels" are not obvious with policies, and users have the lowest tendency to go to the raster units with these two attributes.

As shown in Table 5.1, the competitiveness value of the 5-category details introduced the performance of our proposed RC-GAT model in 24 months. The competitive relationship of each raster unit is based on the frequency of user access to POIs. Compare with the RC-GAT competitiveness training result performance of April (65.58, 24.09, 98.61, 62.08, 35.16) and May (67.06, 26.18, 101.35, 60.75, 33.24) in 2020 which are the stage affected by intervention policies of restricting activities, **the response of user visit category: "transportation" value has strongly reduced and other categories are reduced obviously.**

In 2021, affected by multiple epidemic prevention and control measures, the competitiveness of the "restaurant" category reached the highest of 90.16 in March and the lowest of 56.71 in September. The Kyoto City Government's control measures against COVID-19 are shown as The catering industry shortening its work hours to 8 pm (show as * in Table 5.2), but the impact has been limited in April, June, and October data. On the other hand, affected by the "Go to Eat Campaign" economic promotion policy, the competitiveness results of "restaurants" in October 2020(89.19), November 2020(87.57), December 2020(86.92), and January 2021 (88.45) remain at a high value.

Affected by the "Go to Travel Campaign" economic promotion policy, the categories of "hotel", "transportation", and "attractions" has increased to a certain extent compared with the competitive performance of the previous months. Specific performance as "hotel" is improved from 28.75 (June 2020) to 33.48 (July), 35.29 (August), 34.72 (September), 46.34 (October), 39.16 (November), 38.44 (December), 41.59 (January 2021), and 35.62 (February). The category of "attractions" has also grown slightly and obtained the highest competitiveness 49.07 in October. For the "transportation" category, in Figure 5.6, it has always maintained a high level of competitiveness. Affected by the government's epidemic prevention measures, "transportation" reached the lowest point of 98.61 in April 2020. The "Go to Travel Campaign" policy initially had little impact on the competitiveness of transport, but there was a significant increase in October (179.65), November (183.45), and December (172.08) compare with the previous performance in 2020.

5.5 Conclusion and Discussion

This chapter introduces regional competitiveness with the social media data (from Twitter) and POI data to train fixed-size raster map tiles. POI data is a microcosm of urban facilities, and effectively describes the POI information in different categories. About 4.41 million tweets with location information and geographic coordinates from January 1, 2020, to December 31, 2021, are collected in this application. **Combining the distribution of urban facilities in the location information of POI data, proposed a training method for the regional competitiveness of raster units based on the tweet data and POIs of Kyoto in Japan.** The dynamic changes in regional competitiveness during the spread of the COVID-19 disease in Kyoto are visualized in this chapter. And a set of comparative experiments are completed to the effectiveness of our method. The results show the applied RC-GAT model is better to reflect government policy responses from social media data and compare with ASPPA, GGLR, and ST-GAT

frameworks, RC-GAT is more sensitive to the aggregation of competitiveness within the perspective of the overall map tiles.

Our research provided a new way for functional analysis of map tiles. Through geographic information analysis, POI data distribution, social media text mining, graph neural network, and a series of visualization tools, explored the impact of social media data in 2020 and 2021 on the spread of COVID-19 disease and government policies with the dynamic relationship between functions.

Part III

Summary

Chapter Contents

6.1	Conclusion	59
6.2	Discussion	59
6.3	Future Work	61

6.1 Conclusion

In this thesis, a map rasterized statistics method is proposed combine with geographic information for the classification of POI attributes and Twitter data categories on the map tile. The map raster statistics method and the applications of dynamic POI feature extraction are introduced. The data sets from a user visited POIs and the short text description with geolocation from Twitter are collected to complete the position-related access prediction. POI data with LBSN provide significant geographic information on maps and is utilized to discuss the dynamic characteristics of map tiles as segmented by city roads. We believe that the POI feature training method can increase the depth of the model through feature filtering and non-linear activation and improve the representation ability of the model.

In this thesis, the rasterization map statistics are applied to the actual training task including the POI dynamic changing with map zooming and the response to the COVID-19 epidemic from the government measures. The SZ-GAT and RC-GAT frameworks are proposed for the user access visualization tasks training. From the results of experiments, the POI geo-features from Tweets display the user’s preference at each map zooming level with 5-dimensional Tweet categories and the regional competitiveness provides the map response since COVID-19. The accuracy of the POI prediction results shows that both SZ-GAT and RC-GAT models can complete the classification tasks of the map tiles. The proposed models have a good performance in the user preference on priori geographic feature tiles.

6.2 Discussion

a. Map Zooming Processing

In this application, we discovered that the visual information of the POI with the map-zooming process could reflect user preferences. This method focuses on the dynamic POI change with map zooming, similar to users’ favorite POIs that are always

displayed preferentially while the map is zoomed in. We utilized the zoom level of map tiles to discuss the relation of user-visit history to POI and realized map-zooming training based on location information.

The evaluation results show that the prediction accuracy of test set B is slightly better than that of set A. We examined the tweet attributes as test sets in different data sizes found that the bigger the data size, the greater dispersion of the prediction result and the actual user-preferred POI data. We compared the category composition of the two test sets and found that Set A has numerous "Transportation" and "Restaurant," while Set B has 30% of "Attraction" in the POI-dense cores. Combined with the user-visit frequency, most of the attractions in Kyoto are temples with large areas. Therefore, the higher the frequency of visits to attractions, the more they can be expressed as users' favorite POI during the map-zooming process. We believe that this is related to the user-preference map tiles with different urban facility functionality characteristics and that frequent user access is more representative of the attributes of this map tile.

In addition, the POI features were imported into different platforms, including Google Maps, OpenStreetMap, Bing Map, and Yahoo! Map. The results introduce the four web-map platform prediction accuracy and show that there are only minor differences. The purpose of SZ-GAT training with POIs shown by the multi-platform web-map results is to adopt the proposed model to different map-platform zoom rules. The results of map-zooming levels 1, 2, and 3 are trained on the base map to avoid iterative errors. From the results of zoom level 3, because the POI proportion displayed on the tile is higher than the remaining levels, the training requires minimal cost and resources.

b. Regional Competitiveness Processing

The Japanese government confirmed the country's first case of COVID-19 on January 16th, 2020. The first known case in Kyoto was recorded on January 30th, 2020. As of December 31st, 2020, the total number of infected people in the Kyoto Prefecture was 4,803. By December 31st, 2021, the number became 36,194, increasing by 31,391 people. With the normalization of the spread of COVID-19, the impact of government epidemic prevention policies on the characteristics of POI visits in Kyoto City has gradually become less and less.

In the Twitter data map to the raster competitive phase, the concept of the map tile feature extraction with tweet attributes provides a new perspective for exploring the functions of the raster unit and the spatial pattern of dynamic activities in cities. The sensitivity of social media data to the dynamic changing on the temporal and different map scales has been able to reflect the status of each raster unit feature in real-time. User access data promotes the POI attributes training efficiency with different categories and the discrete tweet location statistics in the entire map tile, to achieve all

positions mapping to the POIs. In addition, social media data with location information and geographic coordinates are more open and practical to analyze and counter user needs for different map tile functions.

In the graph training phase, by combining social media text data with POI geographic distribution information, the category attributes of each raster unit and map tile can be included in the regional competitiveness model. Raster units represent the POI competitive relationships with 5-category tweet attributes. The temporal visualization is based on map tiles and POI categories can be used to explore the spatial model of dynamic dense urban cores.

6.3 Future Work

Geographical information extraction is a new field of map visualization and POI-data analysis. In future work, we plan to apply the MRSS method to dynamic social data changing under the influence of social events.

We hope that our research methods can be used in other types of application scenarios in geographic information in the future, such as the dynamic changes in the social functions of raster units in cities caused by natural disasters, the popularization effect of the government's implementation of urban construction policies, and commercial geographic information provides reliable reasoning directions.

Bibliography

- (1) Crutcher, M.; Zook, M. *Geoforum* **2009**, *40*, 523–534.
- (2) Graham, M.; Zook, M. *Journal of Urban Technology* **2011**, *18*, 115–132.
- (3) Yin, H.; Zhou, X.; Cui, B.; Wang, H.; Zheng, K.; Nguyen, Q. V. H. *IEEE Transactions on Knowledge and Data Engineering* **2016**, *28*, 2566–2581.
- (4) Stefanakis, E. *Go-Geo matics. Magazine of GoGeomatics Canada* **2015**.
- (5) Netek, R.; Masopust, J.; Pavlicek, F.; Pechanec, V. *ISPRS International Journal of Geo-Information* **2020**, *9*, 101.
- (6) Kuhnert, M.; Voinov, A.; Seppelt, R. *Photogrammetric Engineering & Remote Sensing* **2005**, *71*, 975–984.
- (7) Griesner, J.-B.; Abdessalem, T.; Naacke, H. In *Proceedings of the 9th ACM Conference on Recommender Systems*, 2015, pp 301–304.
- (8) Zhu, X.; Zhou, C. In *2009 International Symposium on Information Engineering and Electronic Commerce*, 2009, pp 730–734.
- (9) Utomo, M. N. Y.; Adj, T. B.; Ardiyanto, I. In *2018 International Conference on Information and Communications Technology (ICOIACT)*, 2018, pp 84–89.
- (10) Liu, W.; Lai, H.; Wang, J.; Ke, G.; Yang, W.; Yin, J. *World Wide Web* **2020**, *23*, 131–152.
- (11) Yuan, J.; Chowdhury, P. K. R.; McKee, J.; Yang, H. L.; Weaver, J.; Bhaduri, B. *Scientific data* **2018**, *5*, 180217.
- (12) Yan, X.; Ai, T.; Yang, M.; Yin, H. *ISPRS journal of photogrammetry and remote sensing* **2019**, *150*, 259–273.
- (13) Zhu, D.; Zhang, F.; Wang, S.; Wang, Y.; Cheng, X.; Huang, Z.; Liu, Y. *Annals of the American Association of Geographers* **2020**, *110*, 408–420.
- (14) Andrade, R.; Alves, A.; Bento, C. *ISPRS International Journal of Geo-Information* **2020**, *9*, 493.
- (15) Yuan, Z.; Liu, H.; Liu, Y.; Zhang, D.; Yi, F.; Zhu, N.; Xiong, H. In *Proceedings of the 43rd international ACM SIGIR conference on research and development in information retrieval*, 2020, pp 629–638.
- (16) Xia, Y.; Gao, J.; Cui, B. In *Proceedings of the 30th ACM International Conference on Information & Knowledge Management*, 2021, pp 2191–2200.

- (17) Wang, X.; Ma, Y.; Wang, Y.; Jin, W.; Wang, X.; Tang, J.; Jia, C.; Yu, J. In *Proceedings of The Web Conference 2020*, 2020, pp 1082–1092.
- (18) Bereuter, P.; Weibel, R.; Burghardt, D. In *Multidis-ciplinary Research on Geographical Information in Europe and Beyond Proceedings of the AGILE'2012 International Conference on Geographic Information Science, Avignon*, 2012, pp 74–80.
- (19) Zhang, X.; Ai, T.; Stoter, J.; Zhao, X. *ISPRS Journal of Photogrammetry and Remote Sensing* **2014**, 92, 147–163.
- (20) Dong, G.; Li, R.; Wu, H.; Chen, W.; Huang, W.; Zhang, H. *Expert Systems with Applications* **2022**, 195, 116590.
- (21) Chang, B.; Park, Y.; Park, D.; Kim, S.; Kang, J. In *IJCAI*, 2018, pp 3301–3307.
- (22) Liu, Y.; Pei, A.; Wang, F.; Yang, Y.; Zhang, X.; Wang, H.; Dai, H.; Qi, L.; Ma, R. *International Journal of Intelligent Systems* **2021**, 36, 3174–3189.
- (23) Li, Y.; Chen, T.; Yin, H.; Huang, Z. *arXiv preprint arXiv:2106.15814* **2021**.
- (24) Xie, H.; Li, D.; Wang, Y.; Kawai, Y. In *IEEE/WIC/ACM International Conference on Web Intelligence and Intelligent Agent Technology*, 2021, pp 641–646.
- (25) Bautista-Puig, N.; De Filippo, D.; Mauleón, E.; Sanz-Casado, E. *Publications* **2019**, 7, 12.
- (26) Li, D.; Rzepka, R.; Ptaszynski, M.; Araki, K. *Information Processing & Management* **2020**, 57, 102290.
- (27) Li, D.; Rzepka, R.; Ptaszynski, M.; Araki, K. In *AffCon@ AAAI*, 2019.
- (28) Rafailidis, D.; Kefalas, P.; Manolopoulos, Y. *Expert Systems with Applications* **2017**, 74, 11–18.
- (29) Franke, N.; Von Hippel, E.; Schreier, M. *Journal of product innovation management* **2006**, 23, 301–315.
- (30) Staszkieicz, P.; Chomiak-Orsa, I.; Staszkieicz, I. *IEEE Access* **2020**, 8, 106009–106022.
- (31) Block, P.; Hoffman, M.; Raabe, I. J.; Dowd, J. B.; Rahal, C.; Kashyap, R.; Mills, M. C. *Nature Human Behaviour* **2020**, 4, 588–596.
- (32) Martin, M. E.; Schuurman, N. *Annals of the American Association of Geographers* **2017**, 107, 1028–1039.
- (33) Slamet, C.; Rahman, A.; Sutedi, A.; Darmalaksana, W.; Ramdhani, M. A.; Maylawati, D. S. In *IOP Conference Series: Materials Science and Engineering*, 2018; Vol. 288, p 012039.

- (34) Ginzarly, M.; Roders, A. P.; Teller, J. *Journal of Cultural Heritage* **2019**, *36*, 1–11.
- (35) Athanasis, N.; Themistocleous, M.; Kalabokidis, K.; Papakonstantinou, A.; Soulakellis, N.; Palaiologou, P. *International Archives of the Photogrammetry, Remote Sensing and Spatial Information Sciences* **2018**, *42*, W4.
- (36) Jing, W.; Song, X.; Di, D.; Song, H. *arXiv e-prints* **2021**, arXiv–2101.
- (37) Yuan, Z.; Liu, H.; Liu, Y.; Zhang, D.; Yi, F.; Zhu, N.; Xiong, H. In *Proceedings of the 43rd International ACM SIGIR Conference on Research and Development in Information Retrieval*; Association for Computing Machinery: New York, NY, USA, 2020, pp 629–638.
- (38) Bruna, J.; Zaremba, W.; Szlam, A.; LeCun, Y. *Spectral Networks and Locally Connected Networks on Graphs*, 2013.
- (39) Wang, X.; Girshick, R.; Gupta, A.; He, K. In *Proceedings of the IEEE conference on computer vision and pattern recognition (CVPR)*, 2018, pp 7794–7803.
- (40) Ramachandran, P.; Parmar, N.; Vaswani, A.; Bello, I.; Levskaya, A.; Shlens, J. In *Advances in Neural Information Processing Systems 32*, Wallach, H., Larochelle, H., Beygelzimer, A., d’Alché-Buc, F., Fox, E., Garnett, R., Eds.; Curran Associates, Inc.: 2019, pp 68–80.
- (41) Xia, T.; Lin, J.; Li, Y.; Feng, J.; Hui, P.; Sun, F.; Guo, D.; Jin, D. *ACM Transactions on Knowledge Discovery from Data (TKDD)* **2021**, *15*, 1–21.
- (42) Zhao, K.; Zhang, Y.; Yin, H.; Wang, J.; Zheng, K.; Zhou, X.; Xing, C. In *IJCAI*, 2020, pp 3216–3222.
- (43) Chang, B.; Jang, G.; Kim, S.; Kang, J. In *Proceedings of the 29th ACM International Conference on Information & Knowledge Management*, 2020, pp 135–144.
- (44) Lim, N.; Hooi, B.; Ng, S.-K.; Wang, X.; Goh, Y. L.; Weng, R.; Varadarajan, J. In *Proceedings of the 29th ACM International Conference on Information & Knowledge Management*, 2020, pp 845–854.
- (45) Wang, Y.; Wang, T.; Tsou, M.-H.; Li, H.; Jiang, W.; Guo, F. *Sustainability* **2016**, *8*, DOI: 10.3390/su8111202.
- (46) Scarselli, F.; Gori, M.; Tsoi, A. C.; Hagenbuchner, M.; Monfardini, G. *IEEE transactions on neural networks* **2008**, *20*, 61–80.
- (47) Fu, X.; Zhang, J.; Meng, Z.; King, I. In *Proceedings of The Web Conference 2020*, 2020, pp 2331–2341.
- (48) Veličković, P.; Cucurull, G.; Casanova, A.; Romero, A.; Lio, P.; Bengio, Y. *arXiv preprint arXiv:1710.10903* **2017**.

List of Figures

1.1	The overview of proposed raster statistics method and applications. . . .	5
2.1	The visualization of POIs (black dots) and Twitter data (red dots) on the Kyoto City road map.	8
2.2	The visualization of map layers of the flat web maps.	9
2.3	The process of map tiles extraction from Google Map API.	10
2.4	An example of a basic raster unit (red area) on the Google map tile. . . .	11
3.1	An example of rasterized map tile with feature map extraction process. .	19
3.2	The process of raster unit convolution and cell feature extraction.	20
3.3	The comparative experiment with CNN (A) and GCN (B) training process.	21
4.1	The detail of POI within map zooming on the example of Kyoto Base Map where the map zooming level: $z = 1$ (1:100000), $z = 2$ (1:10000), $z = 3$ (1:1000).	28
4.2	A Google base map tile with POIs zooming process in zoom level 1 and the detail of rasterized tile units zoom-out segmentation.	29
4.3	An example of POIs and Tweets with geolocation on the Google Base Map, where the POIs and Tweets are divided into 5-dimensional categories to provide the trainable POI attribute vectors.	30
4.4	The overview of the SZ-GAT framework contains the Data Preprocessing Block, Map Tile Graph Attention Network Block, and Output Evaluation Block.	31
4.5	The detail of the input POI data set (Attributes, Coordinates, and Raster Unit Information), where A_1 to A_5 donate the POI location attributes in the category of Restaurant, Hotel, Transportation, Attraction, and Shop. lat, lng donates the latitude and longitude of the POIs. The map tile base features are donated by each raster unit's POI positions: flat position (x, y) , zoom level: z , nearest POI distance d , and the number of the raster unit n in tiles.	32
4.6	The process of our proposed method: SZ-GAT including Spatial Block and Zoom Block, the output layer shows the POI graph structures dynamic display in multiple zoom levels. (POI_2 is disappeared in zoom out process, $z = 2, z = 3$)	34

4.7	A case visualization of SZ-GAT prediction results combined with multiple web map zoom levels, where the orange marks are the positive POIs prediction of the SZ-GAT model, the green marks are the negative POIs prediction results, and the blue marks are the prediction results with lost POIs. The accuracy of the prediction results based on the Google Map test set is evaluated by the other web map platforms.	41
5.1	The overview of our proposed raster competitive relationship frameworks with the RC-GAT training model.	44
5.2	The detail of input POI data with P_A : POI attributes from Tweets in 5 categories, P_C : the coordinates of each POI, P_U : POI attributes of each raster unit.	46
5.3	The process of the proposed RC-GAT framework. We input the POI graph structure and raster relationship to extract regional competitiveness and output the map tile feature in monthly 5 categories.	48
5.4	The result of raster competitive relation on the Kyoto City map in January 2020, where figure (a) is the overview of 5 categories, and figure (b) is the detail of "brown": restaurants, "purple": hotels, "red": transportation, "green": shops, "blue": tourist attractions, respectively.	51
5.5	The case detail of the Kyoto Tower map tile dynamic changing in 24 months.	52
5.6	The COVID-19 response sensitivity of Kyoto regional competitiveness based on the RC-GAT model with the data in Table 5.2.	54

List of Tables

3.1	The Prediction Results of Comparative Experiment Between CNN and GCN Models	23
4.1	The POIs Dynamic Zooming Display Prediction Result with 3D-GCN, ASPPA, GGLR, STP-UDGAT, and SZ-GAT training models.	39
4.2	Users' preference POI score from dynamic zooming display prediction result with 3D-GCN, ASPPA, GGLR, STP-UDGAT, and SZ-GAT models.	39
4.3	The Google map prediction result-based evaluation results of the OSM, Bing, and Yahoo! web map platforms.	40
5.1	The performance of the baseline training model: ASPPA, GGLR, ST-GAT and our proposed RC-GAT from January 2020 to December 2021.	53
5.2	The performance of RC-GAT framework regional competitiveness response of COVID-19 from January 2020 to December 2021 with government measures, where "↓" denotes the epidemic control measures, "*" is the unique measure to a category, "↑" represents the economic stimulus packages.	54

Acknowledgements

I am honored to be able to complete my Ph.D. at Kyoto Sangyo University. Data mining based on geographic information and social media is currently the most popular and difficult research direction, and it takes a lot of time and energy to focus on prediction accuracy optimization and application innovation. In the past three years, from the extraction of the most basic geographic information data to the analysis of the mapping of social media data to the map, I am very grateful to Professor Kawai Yukiko for her support in completing my research. For data mining and geographical information analysis fields, this is a brand new course that requires everyone to study and understand carefully.

Thanks to my professor and assistant professor Wang Yuanyuan for listening to me patiently and giving me advice every time. At the same time, I would also like to thank Dr. Li Da and Dr. Yang Yanhan for their help in the basic theory and accompany. At last, thanks to my family for their encouragement and support in making this journey possible. My Ph.D. study life is coming to an end, but my interest for AI will not stop me from studying. In the future, I will continue to contribute at the intersection of geo-relevant text analysis and machine learning.